UNIVERSITY OF CALIFORNIA SAN DIEGO

Investigating the Roles of Mec1 and Rad53 in the S-Phase Checkpoint in *Saccharomyces cerevisiae*

A Thesis submitted in partial satisfaction of the requirements
for the degree

Master of Science

in

Biology

by

Waverly Tseng

Committee in charge:

Professor Victoria Lundblad, Chair
Professor Lorraine Pillus, Co-Chair
Professor James T. Kadonaga

2018

The Thesis of Waverly Tseng is approved, and it is acceptable in quality and form for publication on microfilm and electronically:

_____

_____
Co-Chair

_____
Chair

University of California San Diego

2018

TABLE OF CONTENTS

ACKNOWLEDGEMENTS

Thank you to Vicki Lundblad for allowing me the chance to experience the innovative and unique environment of a genetics lab at the heart of biology research in San Diego. Thank you to John Lubin, a PhD candidate in the Lundblad lab, for your help with the Mec1 experiments. I would also like to show my appreciation for the other members of the Lundblad lab who have never hesitated to help me learn my way around research and the lab.

ABSTRACT OF THE THESIS

Investigating the Roles of Mec1 and Rad53 in the S-Phase Checkpoint in *Saccharomyces cerevisiae*

by

Waverly Tseng

Master of Science in Biology

University of California San Diego, 2018

Professor Victoria Lundblad, Chair
Professor Lorraine Pillus, Co-Chair

The S-phase checkpoint, developed by the cell in response to DNA damage, is critical to maintaining cellular function. The S-phase checkpoint operates through two separate pathways, the DNA damage checkpoint and the

DNA replication checkpoint. Both pathways of the S-phase checkpoint respond to DNA damage in *Saccharomyces cerevisiae*, or budding yeast, through separate mechanisms both relying on two critical kinases, Mec1 and Rad53. My goal in my master's thesis research was to work toward elucidating the details of these two kinases' roles in both pathways of the S-phase checkpoint. To do so, I subjected highly conserved, hydrophobic residues on the surfaces of Mec1 and Rad53 to extensive mutagenesis using a novel technique designed to identify rare separation-of-function mutations, as well as traditional loss-of-function screens. By conducting a thorough genetic screen of the two kinases, I sought to aid efforts in uncovering additional protein factors involved in the S-phase checkpoint and in clarifying how the two different pathways work in conjunction to respond to DNA damage throughout the cell. Determining specifically how Mec1 and Rad53 work within the two pathways can lead to similar discoveries about the DNA damage response pathways in mammalian cells, facilitating the development of future treatments of cancer and other debilitating genetic diseases.

LIST OF SUPPLEMENTARY FILES

LIST OF FIGURES

LIST OF TABLES

INTRODUCTION

Genome Stability

Maintaining the integrity of DNA is critical to proper cellular function. Defects in processes responsible for preserving DNA sequences inevitably result in mutations across the genome, destabilizing the genome and disrupting important cellular processes. This loss of genome stability leads to the loss of DNA integrity, resulting in mutations that encourage the development of system-wide diseases like cancer (1, 2). Genome instability is present in almost all types of cancers and throughout most stages of the disease, though the degree of instability varies widely between different types of cancers (3).

Genome instability constitutes changes in the DNA sequence ranging from single-nucleotide changes to entire chromosome changes (4). DNA-damaging agents can destabilize the genome by introducing these mutations, leading to the development of system-wide diseases such as cancer. Exogenous sources of DNA damage such as X-rays and ultraviolet light are well-studied sources of cancer-causing mutations (5). However, endogenous sources of DNA damage and associated repair mechanisms present throughout regular cellular function may account for most mutations in the genome and thus are primarily responsible for the development of most cancers (6). Repair mechanisms such as non-homologous end joining and homologous recombination have evolved in response to endogenous sources of DNA damage; however, these repair mechanisms can introduce more mutations and further disrupt genome stability (7).

Replication Stress

Stress arising during DNA replication increase the likelihood of stalled or collapsed replication forks and prevent replication from continuing properly, further disrupting genome stability (8). Certain DNA sequences that contain repetitive motifs or form complex conformations in transcription introduce replication stress. In addition, genes highly transcribed during S phase often stall during replication due to the simultaneous presence of replication and transcription machineries on the same DNA sequence, impeding replication fork progression (8). Diminished levels of dNTPs available for use in replication also introduce replication stress (8). Though DNA repair processes react to and alleviate replication stress, these processes can further disrupt genome stability. Though dedicated repair proteins can restart stalled replication forks, these proteins can also potentially introduce undesired mutations or bulky lesions into the DNA, disturbing the integrity of the DNA and further destabilizing the genome (9).

The S-phase Checkpoint

DNA replication stress is an inevitable side effect of the normal replication process; the S-phase checkpoint has evolved in response to this condition. In order to respond to replication stress, the S-phase checkpoint constantly controls replication rate within S phase through two methods: by slowing down or stopping replication to allow repair of the replication fork, and by preventing chromosomes from segregating when affected by DNA damage (8, 10, 11). These two events typically occur in conjunction; as a result, mutations arising from replication stress

or DNA damage are addressed with minimal disruption to overall genome integrity (8, 11). In addition to responding to replication stress, the S-phase checkpoint also induces transcription of key DNA damage response genes and inhibits mitosis until replication is resumed and completed (11, 12). Through these functions, the S-phase checkpoint stabilizes the replication fork and thus prevents genome instability (12).

Many studies investigating the S-phase checkpoint have used *Saccharomyces cerevisiae*, or budding yeast, as their model organism of choice. *S. cerevisiae* has many advantages for genetic research, a primary one being the ease with which yeast gene expression can be manipulated and observed (13). In addition, the *S. cerevisiae* genome was the first eukaryotic genome to be comprehensively sequenced; knowledge about the *S. cerevisiae* genome has only been expanded upon further with time (14). As a result, many yeast genes with mammalian homologs have been identified (15). Critical cellular processes involving these genes are often functionally conserved through eukaryotes (16); studies in yeast genes have thus helped clarify the roles of their mammalian homologs in essential cellular processes common to both species, such as DNA mismatch repair (17, 18). In this way, investigating genes essential to a certain process in yeast can lead to discoveries about genes essential to the same process in humans. As proteins critical to the S-phase checkpoint and the checkpoint itself are conserved in eukaryotes, studying these checkpoint proteins in *S. cerevisiae* can potentially reveal new information about the functions of these

proteins and this essential response to DNA damage in both yeast and humans (10).

The DNA Damage and DNA Response Checkpoints

The S-phase checkpoint consists of two distinct pathways: the DNA damage checkpoint (DDC) and the DNA replication checkpoint (DRC) (Fig. 1). The DDC responds to DNA damage throughout the cell cycle and maintains the integrity of DNA through normal cellular processes, such as cell division (19). The DRC, which exists alongside and separate from the DDC, specifically recognizes arrested replication forks and primarily functions during S phase of the cell cycle (20). In addition, the activation of Rad53 in the DDC differs from the activation of Rad53 in the DRC; whereas the DDC responds slowly and continuously, the DRC responds quickly and briefly (11). The combination of these two patterns of activation therefore makes the S-phase checkpoint situationally flexible, as it has both long-term and short-term responses to different types of DNA damage or replication stress (11).

Two proteins critical to both pathways of the S-phase checkpoint in *S. cerevisiae* are Mec1, a sensor kinase, and Rad53, an effector kinase. Although there are differences between the specific mechanisms of the two pathways, Mec1 activates Rad53 in both pathways through a phosphorylation cascade in response to DNA damage and replication stress (21, 22). Mec1 helps stabilize the replication fork in a manner independent from Rad53; however, both proteins are important to preventing stalled forks from breaking down irreversibly in conditions of DNA

damage (23). In addition, both proteins are necessary in regulating the rate of replication, a constant function of the S-phase checkpoint (10). In regulating the rate of replication, the Rad53 and Mec1 kinases promote several cellular processes (including dNTP production, the transcription of DNA damage response genes, and the restart or repair of arrested or damaged replication forks) and inhibit others (including cell cycle progression) (11).

Although some details of the two checkpoint pathways are known, the mechanisms through which Mec1 and Rad53 operate are still poorly understood. In the DDC, Mec1 activates Rad53 through a mediator protein Rad9. After DNA damage, Mec1 recruits Rad53 to the site of DNA damage by phosphorylating Rad9. Rad53 is then hyperphosphorylated by Mec1 and activated, a process that is necessary for Rad53's catalytic activation (11, 22). Rad9 is known to promote Rad53's activation by Mec1 and autophosphorylation (11). In addition, the mediator Rad9 is necessary for Rad53 to be activated; studies have shown that Mec1 is less efficient in activating Rad53 when acting alone, indicating that Rad9 is a necessary catalyst for this key phosphorylation cascade to occur (24).

In contrast, the DRC appears to operate with a different mechanism involving a different mediator protein, Mrc1. Although Mec1 is known to recruit Rad53 in response to disruptions in replication by phosphorylating Mrc1, not much is known about this process (11). Some researchers have hypothesized that Mec1 may phosphorylate Mrc1 to catalyze Rad53 activation in a similar way to its phosphorylation of Rad9 (20); others propose that Mrc1 may promote Mec1 to

directly activate Rad53 (25), or that Mrc1 otherwise modulates the sensitivity of Rad53 to DNA damage signals (26). Although both Mrc1 and Rad9 appear to function similarly as mediator proteins by promoting the association of Mec1 and Rad53, the mechanism Mrc1 acts through remains poorly understood in comparison to that of Rad9 (27).

Despite the difference in knowledge of each of these pathways, it can still be surmised that the differences between the two pathways seem to lie in the mechanism through which the respective mediator proteins activate Rad53, rather than in the effect on Rad53 activity (11). While Mrc1 is necessary in the DRC to activate Rad53 in response to DNA replication stress, Rad9 is not; however, the reason for such a difference has not been determined (19). By elucidating the mechanisms behind each checkpoint pathway, the different functions of each pathway can be better understood and can lead to new discoveries about the critical cellular response to DNA damage.

Identifying the Roles of Mec1 and Rad53 in the S-phase Checkpoint

The above discussion argues that the mechanisms through which the S-phase checkpoint operate remain poorly understood. Namely, the roles of two critical proteins, Mec1 and Rad53, in the DNA damage response pathways have been difficult to characterize in detail because both proteins are derived from essential genes (28). Essential genes, which are genes essential to the overall function of the cell, are difficult to study, as null mutations interfering with the gene's essential function result in lethality (29). As essential genes, Mec1 and Rad53 are

much less amenable to the goal of studying gene function and are still poorly understood. Because of this gap in knowledge, I focused my master's thesis research on studying these two proteins and their roles in the DNA damage response pathways of the S-phase checkpoint. To do so, I primarily used a novel mutagenesis assay designed by the Lundblad lab to identify rare separation-of-function mutations, or mutations resulting in the loss of a single biochemical property (30). By using this assay alongside traditional mutagenesis assays, I sought to create functional surface maps of Mec1 and Rad53 that could provide new insight into additional protein factors involved in the response to DNA damage in yeast. By characterizing these two proteins critical to both DNA damage response pathways of the S-phase checkpoint in yeast, I hope to contribute to the understanding of the corresponding pathways in humans and thus facilitate the development of future treatments of cancer and other debilitating genetic diseases (11, 9).

MATERIALS AND METHODS

Strains and Plasmids

All overexpression dominant-negative genetic screens of *MEC1* and *RAD53* used two strains, YVL3658 (*MAT***a** *cdc13*-S611L *bar1*Δ::cNAT *ura3*-52 *lys2*-801 *trp1*-Δ1 *his3*-Δ200 *leu2*-Δ1) and YVL3660 (*MAT***a** *cdc13*-F684S *bar1*Δ::cNAT *ura3*-52 *lys2*-801 *trp1*-Δ1 *his3*-Δ200 *leu2*-Δ1). Each *cdc13-ts* strain provides a different range of analysis at different temperatures. These strains were transformed with high-copy 2μ *LEU2* plasmids expressing wild-type or mutant *MEC1* or *RAD53* genes expressed from the *ADH* promoter. The plasmids used for these overexpression dominant-negative genetic screens were pVL7717 (2μ *LEU2 ADH-MEC1*) for Mec1 and pVL7719 (2μ *LEU2 ADH-RAD53*) for Rad53. The synthetic lethality and telomere length assays in *MEC1* and *RAD53* used the shuffle strains YVL5404 (*MAT***a** *mec1*-Δ::KAN *ura3*-52 *lys2*-801 *trp1*-Δ1 *his3*-Δ200 *leu2*-Δ1) and YVL5405 (*MAT***a** *rad53*-Δ::NAT *ura3*-52 *lys2*-801 *trp1*-Δ1 *his3*-Δ200 *leu2*-Δ1), respectively. These strains were transformed with single-copy *CEN LEU2* plasmids expressing wild-type or mutant *MEC1* or *RAD53* genes expressed from the native promoter. The plasmids used for these loss-of-function genetic screens were pVL7737 (*CEN LEU2 MEC1*) for Mec1 and pVL7740 (*CEN LEU2 RAD53*) for Rad53. QuikChange mutagenesis was used to introduce missense mutations into Mec1 and Rad53. The standard lithium acetate method was used to introduce plasmids into yeast (31).

Overexpression Dominant-Negative Mutagenesis Assay

Plasmids expressing mutant alleles of Mec1 (derived from pVL 7717) or Rad53 (derived from pVL7719) were transformed into YVL3658 or YVL3660, respectively, and were grown at room temperature on selective agar media selecting for only transformants that have accepted the mutant alleles (32). Once grown, single colonies were picked and grown to saturation in selective liquid media for 3 overnight periods at room temperature. 200μl from each culture were then transferred into microtiter dishes and plated onto selective agar media using five-fold serial dilutions. These plates were grown at varying temperatures for five days. Growth was photographed on the second, third, and fourth days of growth.

Loss-of-Function Assays

Plasmids expressing mutant alleles of Mec1 (derived from pVL7737) or Rad53 (derived from pVL7740) were transformed into YVL5404 or YVL5405, respectively, and were grown at 30°C on selective agar media. Following this, mutants were put through two variations of the synthetic lethality protocol and the telomere length protocol:

Synthetic Lethality

Single colonies were picked and grown to saturation in rich liquid media for 1 overnight period at 30°C. 200μl from each culture were serially diluted as before and plated onto agar media containing varying concentrations of hydroxyurea (made by diluting a stock solution of 0.65M HU with rich media) or methyl

methanesulphonate (made by diluting a stock solution of 99% MMS with rich media). Hydroxyurea (HU) and methyl methanesulphonate (MMS) are both DNA damaging agents that introduce replication stress into the cell; HU, which depletes cells of dNTPs necessary for replication, and MMS, which stalls replication forks, can thus be used in synthetic lethality assays as sources of DNA damage to test the effect of disruptive mutations on the cell's ability to respond to DNA damage (33, 34). These plates were grown at 30°C for two days. Growth was photographed on the second day of growth.

Single colonies arising only from the transformation of plasmids into YVL5405 were also picked and grown to saturation in selective liquid media for 2 overnight periods at 30°C. 200μl from each culture were serially diluted as before and plated onto agar media containing 5-fluro-orotic acid (5-FOA). 5-FOA, following conversion by an enzyme naturally found in yeast cells, is toxic to the cell, and thus can be used to enhance the effect of disruptive mutations on the cell's ability to respond to DNA damage for easier detection (35). These complete mixture (CM) 5-FOA plates were grown for six days at 30°C. Growth was photographed on the third and sixth days of growth.

Telomere Length Assay

Single colonies were picked and streaked onto selective agar media containing 5-FOA. After three days of growth at 30°C, single colonies from each streakout were picked and streaked onto selective agar media. After three days of

growth at 30°C, single colonies from each streakout were picked and streaked onto rich agar media for ~100 generations at “3x” streakouts. Two independent single colonies from the “3x” streakouts were then picked and grown to saturation in rich media for 1 overnight period at 30°C. Genomic DNA was purified and prepared using the Wizard Genomic DNA Purification Kit (Promega) and digested with Xho1 enzyme (New England Biolabs). Samples were separated on 20-cm 0.8% gels, transferred overnight on a nylon membrane (Amersham Hybond N+), and probed with poly d(GT/CA).

CHAPTER 1: CREATING FUNCTIONAL SURFACE MAPS OF *MEC1* AND *RAD53*

My goal in my master's research was to investigate the roles of Mec1 and Rad53 in the DNA damage response pathways of the S-phase checkpoint. Mec1 and Rad53, as discussed earlier, are essential genes in yeast; due to the difficulty of studying these genes, the exact roles of Mec1 and Rad53 in the S-phase checkpoint are poorly understood. Traditional mutagenesis assays employed in studying essential genes are forward mutagenesis screens in which the genetic basis of a phenotype is determined after already observing the phenotype. These screens are generally effective at uncovering mutations that confer loss-of-function (LOF) phenotypes, or mutations that show a phenotype due to reduced or abolished protein function (36). However, these traditional loss-of-function assays rely on certain factors that can be unpredictable and unreliable, especially when working with essential genes. These assays typically work by reducing or abolishing protein function through deletion of the gene of interest; as a result, these assays are unsuitable for studying essential genes, as such a deletion would lead to lethality (29). Furthermore, loss-of-function assays typically utilize genetic reagents that disrupt many factors in addition to the target biochemical activity (37). This pleiotropic effect complicates the identification of mutations that show LOF phenotypes, as these phenotypes could result from a mutation unfolding the protein and the consequent disruption of multiple biochemical activities (30, 38). In addition, traditional loss-of-function assays typically mutate highly conserved

residues to alanine based on the reasoning that alanine mutations are less disruptive to protein structure (39); however, such mutations could potentially miss functionally important amino acids (30, 40).

To avoid these limitations, the technique of overexpression dominant-negative (ODN) mutagenesis can be used. The ODN mutagenesis assay, a novel technique developed by the Lundblad lab, is designed to identify rare separation-of-function mutations. Unlike traditional loss-of-function assays, the ODN assay retains the endogenous gene in addition to overexpressing the mutant gene. Because the endogenous gene is still present, the assay avoids showing phenotypes for mutations that result in unfolded or destabilized proteins, preventing the false identification of mutations that do not actually affect specific biochemical activities (30). As a result, if a mutation results in an overexpression dominant-negative (ODN) phenotype (Fig. 2), the mutant protein is assumed to be properly folded and functionally able to displace and disrupt the activity of the endogenous protein when overexpressed (30).

The ODN assay can be used effectively in reverse mutagenesis screens to identify functionally important residues. Unlike forward mutagenesis screens typically involving traditional loss-of-function assays, reverse mutagenesis screens test the effects of select mutations on the activity of a protein (41). Reverse mutagenesis is thus advantageous for identifying separation-of-function mutations, as functionally important amino acids on the surfaces of proteins can be selectively mutated and tested through the ODN assay. Surface residues are more likely to

be involved in biochemical activity; in addition, if the amino acids are highly conserved, the resulting missense mutations are more likely to disrupt specific biological functions and thus confer an ODN phenotype (42). Mutating these highly-conserved surface residues to the opposite charges can further disrupt specific biochemical activity and show a corresponding phenotype (42). This process of charge-swap mutagenesis can be applied to the surface of a protein to generate a large number of mutations that potentially disrupt specific biochemical activities. By selecting highly conserved, hydrophobic surface residues and testing the effects of charge-swap mutations in yeast strains "sensitized" to certain defects in genome stability, rare separation-of-function mutations can be more effectively identified (30). By using sensitized strains to identify these separation-of-function mutations, we can work toward understanding not only the role of the studied protein in a certain biochemical activity or pathway, but also the protein's role in maintaining genome stability (30).

The ODN assay is also useful in identifying different types of separation-of-function mutations. Mutations resulting in ODN phenotypes typically show diminished growth when introduced into these strains, suggesting that these mutations could potentially interfere with the protein of interest's normal function in the cell (Fig. 2). However, we have also identified mutations that suppress the growth phenotype of *cdc13-ts* yeast strains sensitized to defects in telomere regulation. These mutations, when introduced into these *cdc13*-defective strains, show enhanced growth in what the Lundblad lab has named the Roc$^-$ (rescue of

CDC13) phenotype, indicating a possible “rescue” of the *cdc13-ts* strain to levels beyond that of the wild-type protein (Fig. 3). The ODN protocol thus facilitates the identification of amino acids that are potentially important sites of interaction between the two proteins and associated proteins in the DNA damage response pathways of the S-phase checkpoint.

The overexpression dominant-negative (ODN) assay is thus effective in generating functional surface maps of Mec1 and Rad53 (42). These maps, constructed by identifying every amino acid on the surface of each protein that is required for function, can lead to greater knowledge about the interactions between these two proteins and other associated protein complexes (43, 44). As discussed earlier, the ODN assay can be used to more effectively study the two essential genes Mec1 and Rad53, as the assay does not involve deletion of the gene of interest. However, a variation of traditional loss-of-function assays can be useful in construction of these functional surface maps of Mec1 and Rad53. By mutating highly conserved, hydrophobic amino acids on the surfaces of each protein and assessing the effects of those mutations through both the overexpression assay and the loss-of-function assay, I can broaden the scope of my genetic screen of Mec1 and Rad53. By comparing the effect of a certain mutation through a combination of these two assays in my master’s thesis research, I can more thoroughly work to determine the roles of Mec1 and Rad53 in the S-phase checkpoint.

CHAPTER 2: GENETIC ANALYSIS OF *MEC1*

Highly conserved, hydrophobic amino acids on the surface of Mec1 were chosen for mutagenesis and mutated to the opposite charge. In order to better identify potential separation-of-function mutations in Mec1, I tested the generated mutations through the overexpression dominant-negative mutagenesis screen and in the loss-of-function (LOF) mutagenesis screen (Table S1). Both screens utilized different conditions of DNA damage or replication stress in testing the response of the mutant protein. I also assessed the telomere length of each mutant protein generated in the LOF screen.

Chapter 2.1: ODN Mutagenesis

As discussed earlier, the overexpression dominant-negative (ODN) mutagenesis screen is an effective technique for identifying potential separation-of-function mutations in the essential gene Mec1. In collaboration with John Lubin, a PhD candidate in the Lundblad lab, I generated a panel of surface residue mutations and introduced these mutations into two *cdc13-ts* strains “sensitized” to telomere regulation defects, the use of which enhances any phenotypes present (45). Then, through the ODN assay, I assessed the effect of each mutation on the cell’s overall ability to respond to replication stress at increasingly restrictive temperatures (Table S1). Out of the 125 mutations tested in this screen, 28 presented a notable overexpression dominant-negative (ODN) phenotype, with either increased or decreased growth at restrictive temperatures (Table 1).

Phenotypes were determined by comparison with *mec1* mutations that present wild-type like growth; because most mutations will not affect biochemical activity of the protein, the phenotype most *mec1* mutations exhibit can be used as a "representative wild type." Of these 28 mutations, when compared to representative wild-type growth, 3 showed diminished growth with typical ODN phenotypes at restrictive temperatures, while 25 showed enhanced growth with Roc$^-$ phenotypes at restrictive temperatures (Fig. S1). Fig. 4 shows a range of these ODN phenotypes exhibited at restrictive temperatures, as assessed in my ODN screen.

Chapter 2.2: LOF Mutagenesis

Traditional loss-of-function (LOF) mutagenesis screens can be used alongside ODN mutagenesis to construct a thorough functional surface map of Mec1. Again in collaboration with John Lubin, I generated the same panel of mutations and introduced these mutations into a *mec1*-Δ strain. Then, through the synthetic lethality assay, I assessed the effect of each mutation on the cell's ability to survive in conditions of DNA damage and replication stress (Table S1). Through the telomere length assay, I assessed the effect of each mutation on telomere length (Table S1).

Synthetic Lethality

In the synthetic lethality assay, I assessed the effects of *mec1* mutations on the cell's overall ability to respond to different types of DNA damage and replication

stress. In doing so, varying concentrations of HU and MMS were used to better gauge the strength of any resulting phenotypes. Out of the 118 mutations tested in these assays, 22 presented notable phenotypes in response to these conditions of DNA damage and replication stress (Table 2, Fig. 5).

These 118 *mec1* mutations were also subjected to 5-fluoro-orotic acid (5-FOA), a genotoxic agent that challenges cell viability, during telomere length analysis. Though the effects of these mutations on the cell's ability to respond to 5-FOA were not formally assayed, 13 out of the 118 mutations assayed showed either significantly diminished growth or inviability (Table 2).

Telomere Length

In the telomere length assay, I assessed the effects of *mec1* in *mec1-*Δ strains on telomere length. However, of the 116 mutations assessed in this assay (Fig. S2), only 4 showed a slight difference in telomere length (Fig. 6, Table 3). As noted earlier, 2 of these 116 mutations put through the telomere length assay were inviable on 5-FOA (Table 2). These 2 mutations were thus unable to be assessed for telomere length phenotypes.

CHAPTER 3: GENETIC ANALYSIS OF *RAD53*

As in the genetic analysis of Mec1, highly conserved, hydrophobic amino acids on the surface of Rad53 were selected and mutated to the opposite charge (Table S2). These generated mutations were tested through the overexpression dominant-negative mutagenesis screen and in the loss-of-function (LOF) mutagenesis screen, in varying conditions of DNA damage or replication stress. I also assessed the telomere length of each mutant protein generated in the LOF screen.

Chapter 3.1: ODN Mutagenesis

The overexpression dominant-negative (ODN) screen can also be used to identify possible separation-of-function mutations in Rad53. As before, I generated a panel of surface residue mutations and introduced them into the same two *cdc13-ts* strains. The effect of each mutation on the cell's overall ability to respond to replication stress at increasingly restrictive temperatures was again assessed through the ODN assay (Table S2). Out of the 78 mutations tested in this screen, 25 presented a notable overexpression dominant-negative (ODN) phenotype, 4 with a typical ODN phenotype of decreased growth and 21 with a Roc^- phenotype of increased growth at restrictive temperatures compared to the wild type (Table 4, Fig. S3). Fig. 7 shows a range of these ODN phenotypes exhibited at restrictive temperatures, as assessed in my ODN screen.

Chapter 3.2: LOF Mutagenesis

Using the same techniques as in the genetic analysis of Mec1, I generated the same panel of mutations and introduced these mutations into a *rad53*-Δ strain. Again, I used the synthetic lethality and telomere length assays to assess the effects of these mutations on the cell's ability to survive in conditions of DNA damage and replication stress, as well as the effects on telomere length, respectively (Table S2).

Synthetic Lethality

In the synthetic lethality assay, I used hydroxyurea (HU), methyl methanesulfonate (MMS), and 5-fluoro-orotic acid (5-FOA) to assess the effects of *rad53* mutations on the cell's viability in conditions of DNA damage and replication stress. Varying concentrations of HU and MMS were again used to better gauge the strength of any resulting phenotypes; the concentration of 5-FOA was held constant. Out of the 83 mutations tested in these assays, 20 presented notable phenotypes in response to any of these three conditions of DNA damage and replication stress (Table 5, Fig. 8).

Telomere Length

As before, I assessed the effects of mutations in Rad53 in *rad53*-Δ strains on telomere length. Of the 69 mutations assessed in this assay (Fig. 9), none showed any notable effect on telomere length.

FIGURES

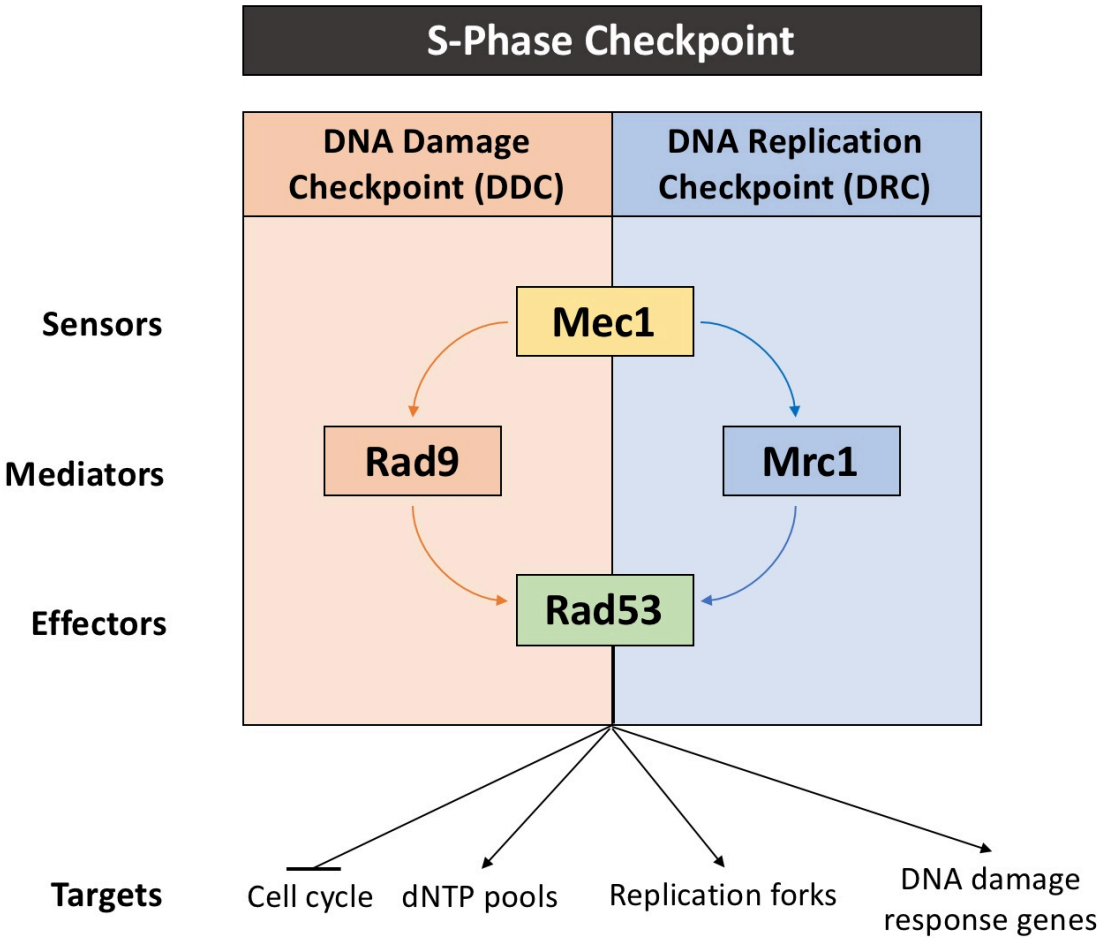

Figure 1. The S-phase checkpoint. Simplified summary of the two major pathways in the S-phase checkpoint, the DNA damage checkpoint and the DNA replication checkpoint. Adapted from Fig. 1 in (11), although this pathway appears in many S-phase checkpoint papers.

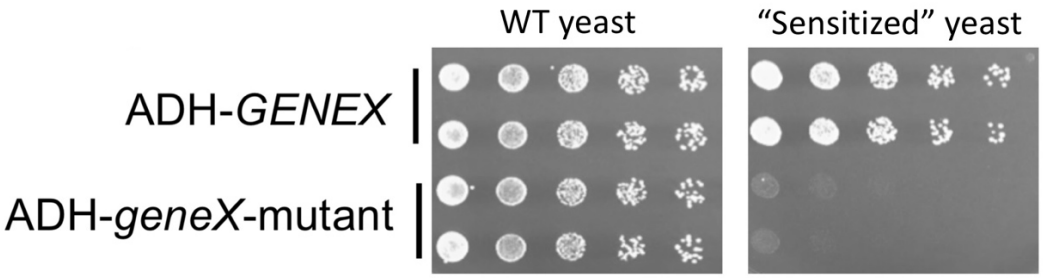

Figure 2. An example result from an ODN mutagenesis experiment. Comparison between a wild-type control and a "Gene X" mutant. This is a representative example of many ODN experiments performed by the Lundblad lab.

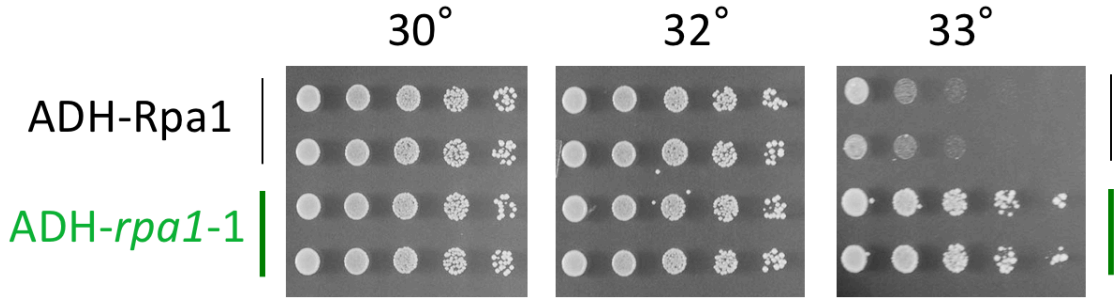

Figure 3. An example of a Roc$^-$ phenotype. Comparison of growth at increasingly restrictive temperatures between a wild-type control and a mutation conferring a Roc$^-$ (rescue of CDC13) phenotype in a *cdc13-ts* yeast strain. Work in Rpa1 done by Corinne Moeller, a graduate student in the Lundblad lab. This is a representative example of a strong Roc$^-$ phenotype that has also been found in ODN screens of other proteins.

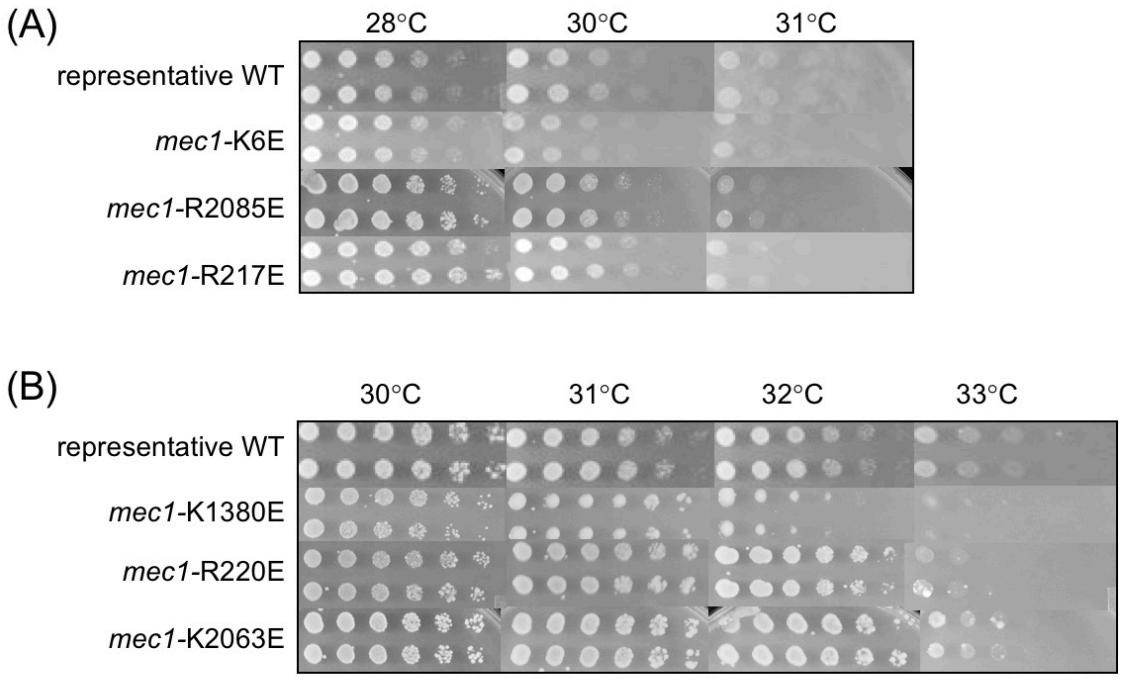

Figure 4. Representative ODN phenotypes exhibited by *mec1* mutations. Growth of yeast strains (A) YVL3658 (*cdc13*-S611L) and (B) YVL3660 (*cdc13*-F684S) at increasingly restrictive temperatures, transformed with high-copy plasmids expressing the indicated *mec1* mutations from an ADH promoter. Pictures shown were taken on the third day of growth. Representative wild-type control shown is a *mec1* mutation with average "wild-type-like" growth. Preliminary results.

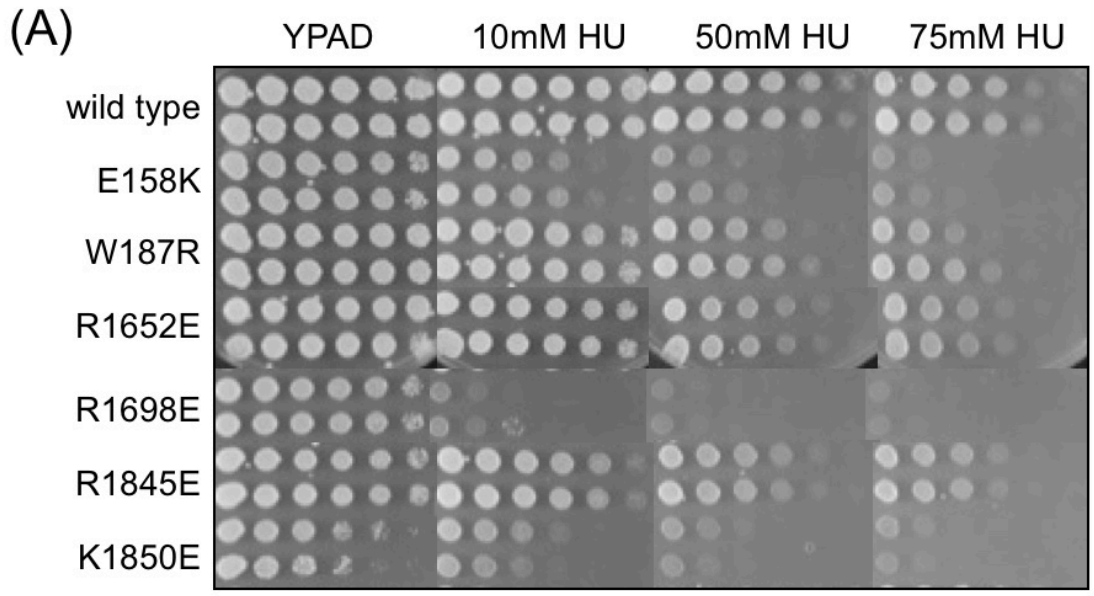

Figure 5. Phenotypes exhibited by *mec1* mutations resulting from conditions of DNA damage and replication stress. Growth of yeast strain YVL5404 (*mec1-*∆), transformed with single-copy plasmids expressing either wild-type *MEC1* or the indicated *mec1* mutations from a native *MEC1* promoter, on (A) HU and (B) MMS plates. Pictures shown were taken on the sixth day of growth. Preliminary results.

Figure 5 (continued).

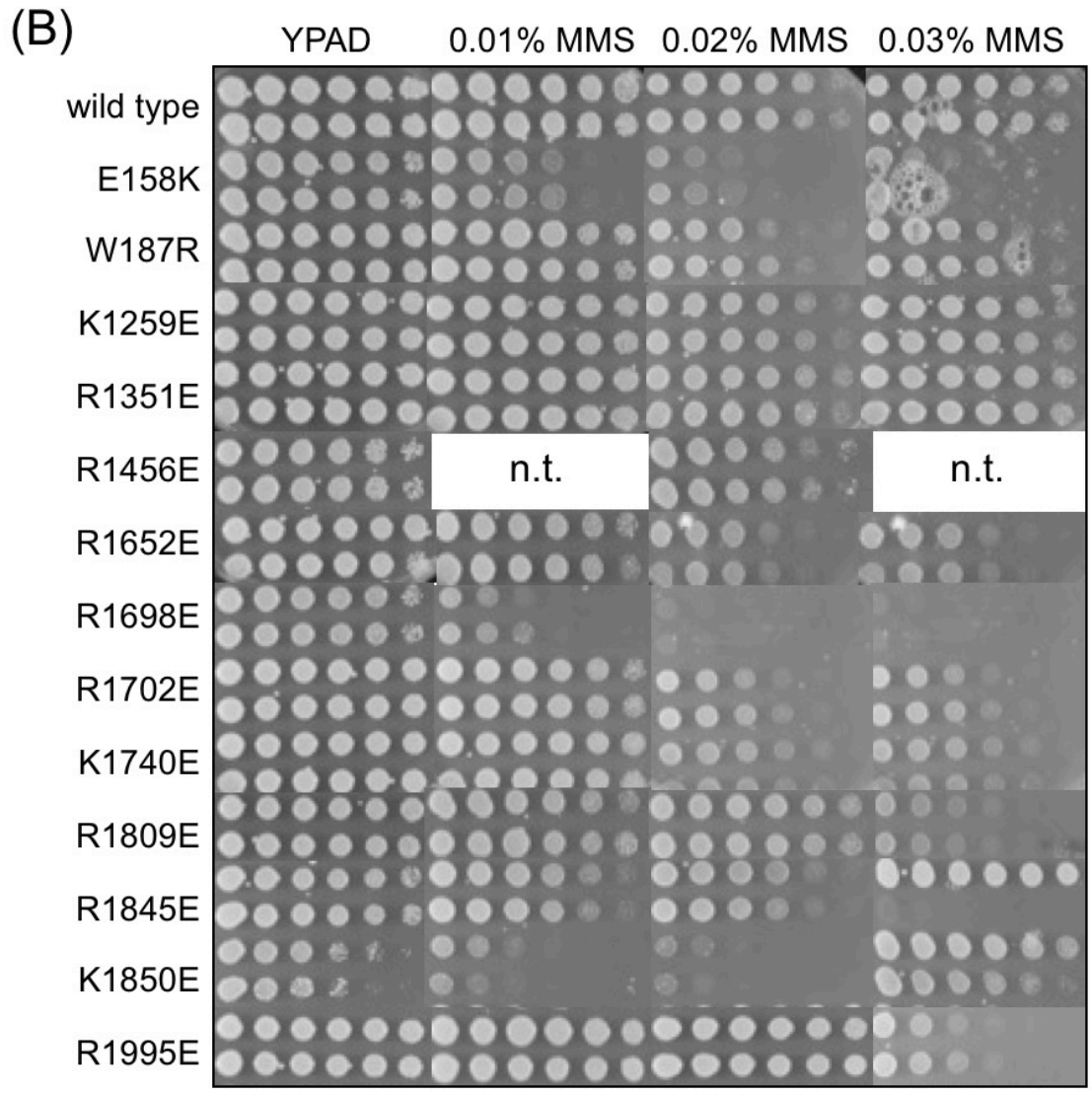

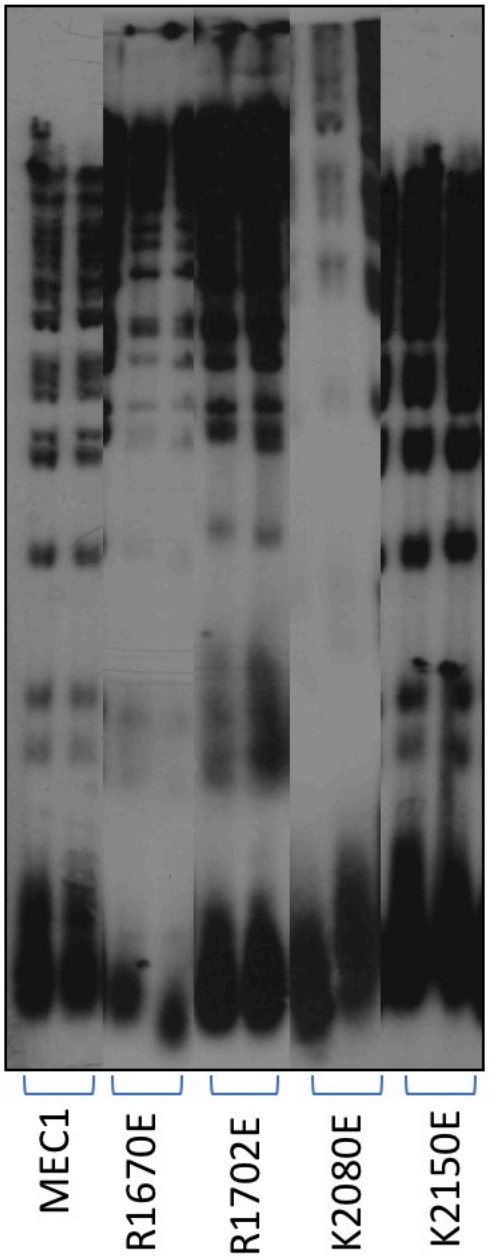

Figure 6. Telomere length phenotypes exhibited by *mec1* mutations. Telomere length of *mec1*-Δ strains transformed with single-copy plasmids expressing either wild-type *MEC1* or the indicated *mec1* mutations from the native *MEC1* promoter. Assessed after ~100 generations of growth.

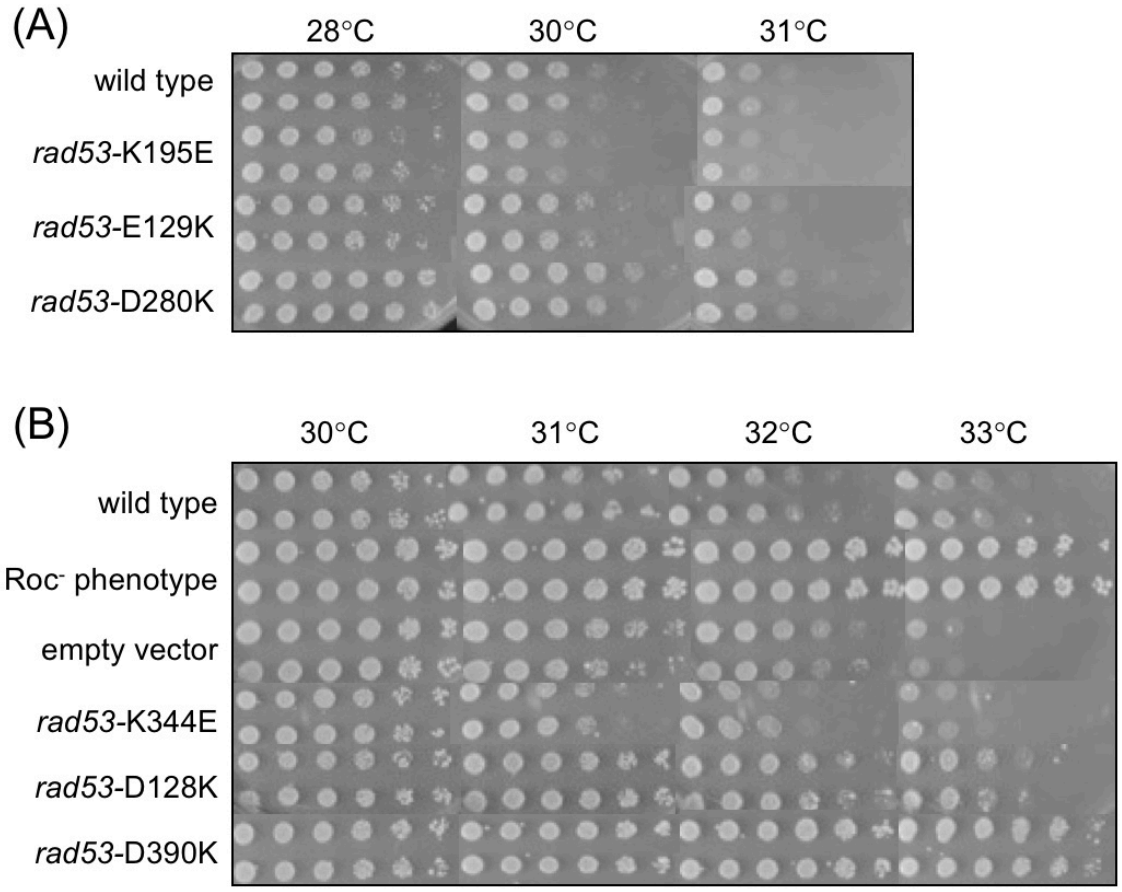

Figure 7. Representative ODN phenotypes exhibited by *rad53* mutations. Growth of yeast strains (A) YVL3658 (*cdc13*-S611L) and (B) YVL3660 (*cdc13*-F684S) at increasingly restrictive temperatures, transformed with high-copy plasmids expressing either wild-type *RAD53* or the indicated *rad53* mutations from an ADH promoter. The Roc- phenotype control used was from a mutation in Rpa1, constructed by Corinne Moeller, a graduate student in the Lundblad lab. Pictures shown were taken on the third day of growth.

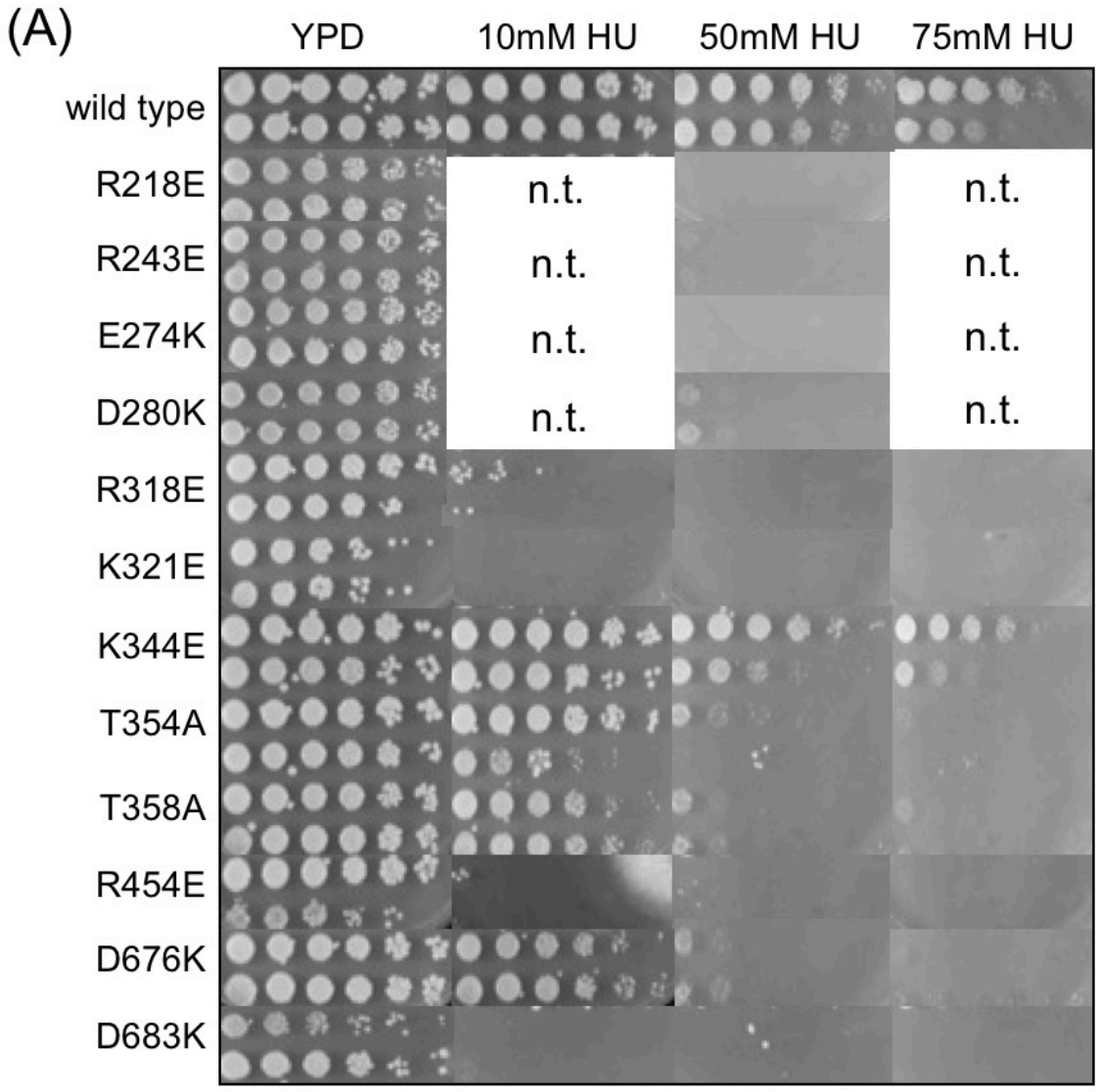

Figure 8. Phenotypes exhibited by *rad53* mutations resulting from conditions of DNA damage and replication stress. Growth of yeast strain YVL5405 (*rad53*-Δ), transformed with single-copy plasmids expressing either wild-type *RAD53* or the indicated *rad53* mutations from a native *RAD53* promoter, on (A) HU, (B) MMS, and (C) complete mixture (CM) 5-FOA plates. Most pictures shown were taken on the sixth day of growth. Preliminary results.

*Pictures for indicated mutations were taken on fourth day of growth.

Figure 8 (continued).

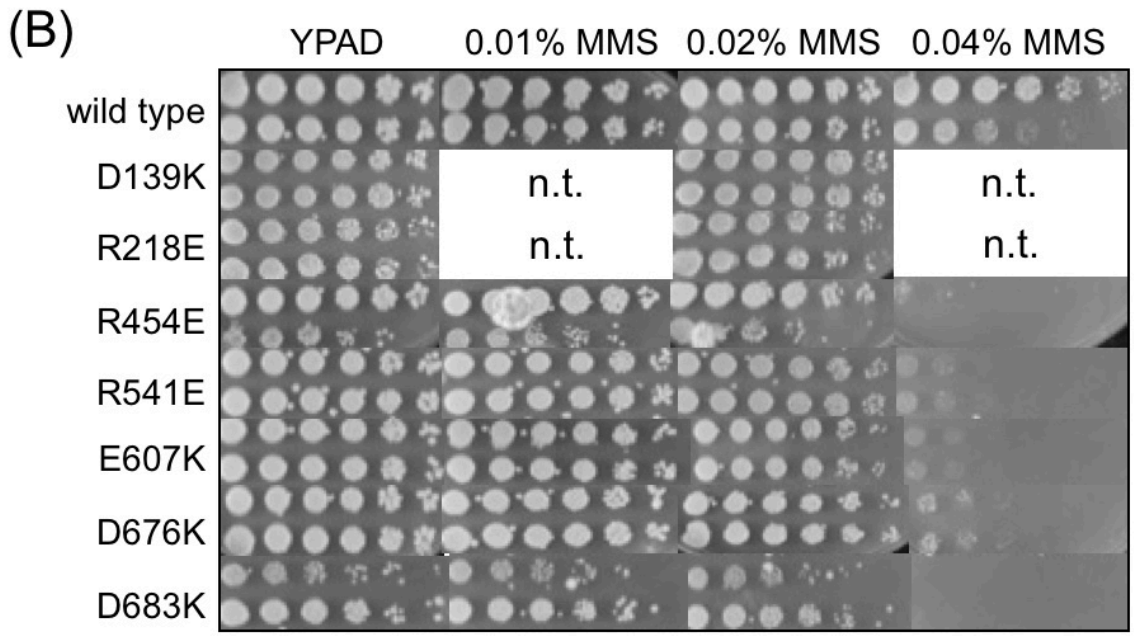

Figure 8 (continued).

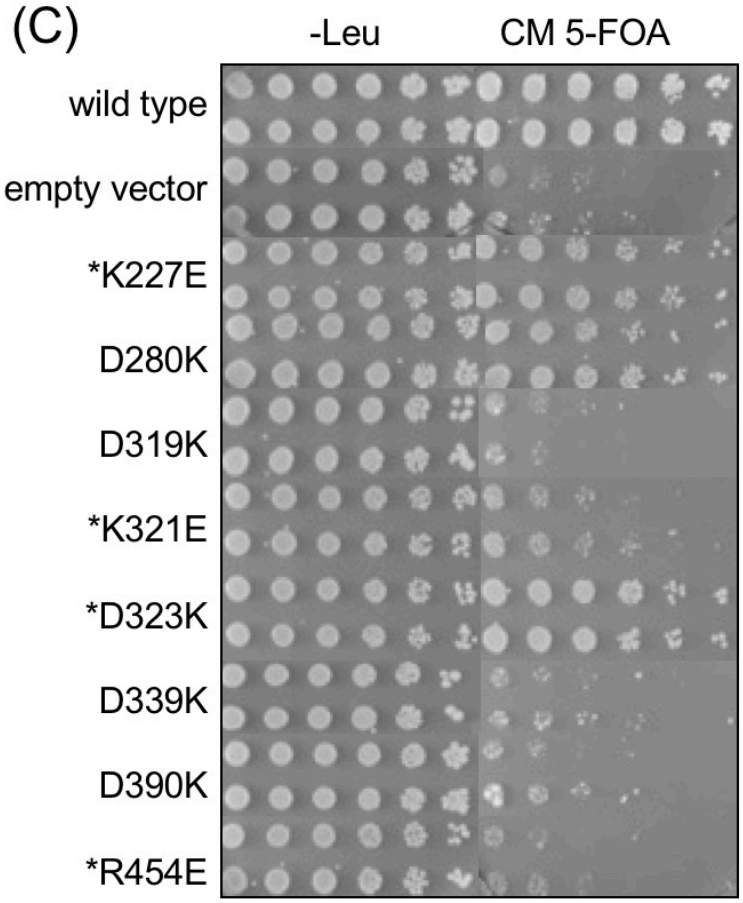

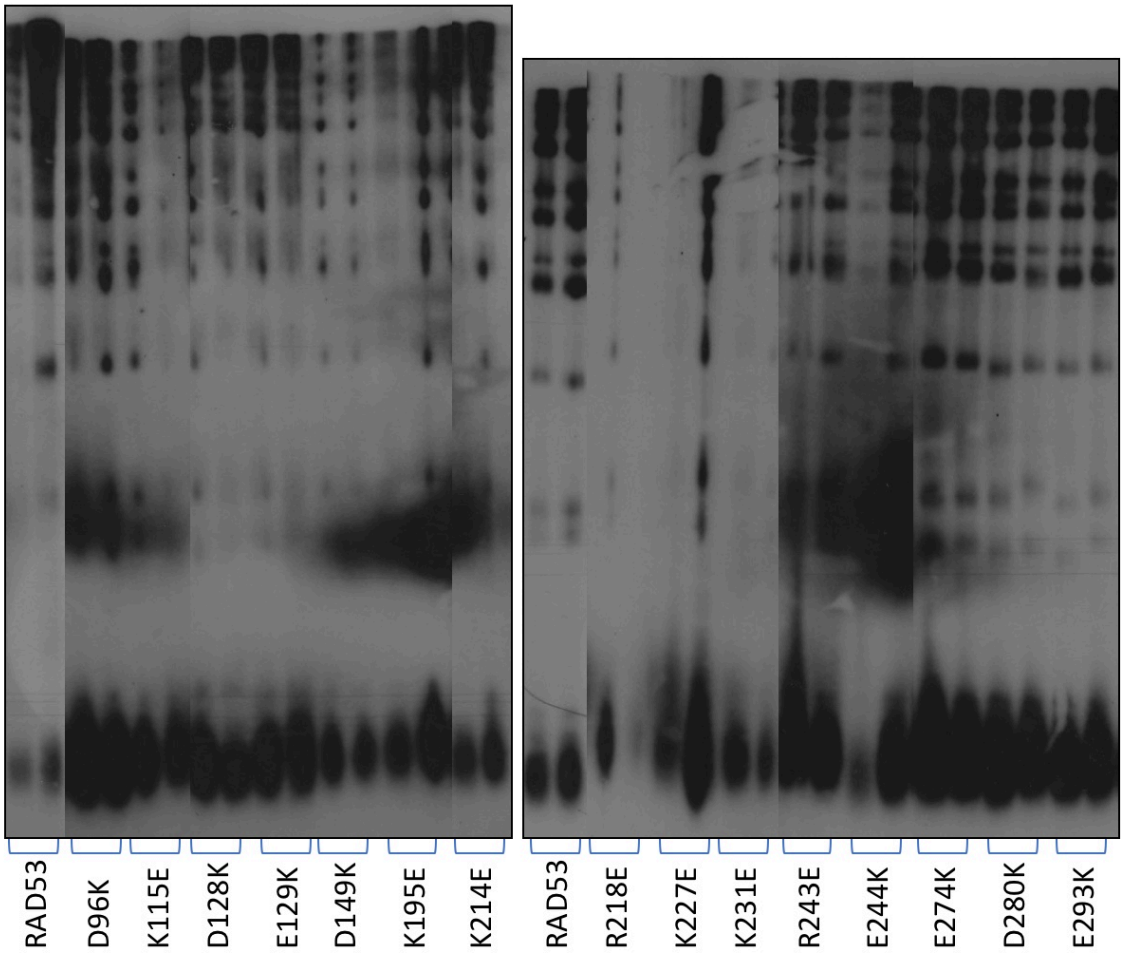

Figure 9. Telomere length analysis of *rad53* mutations. Telomere length of *rad53*-Δ strains transformed with single-copy plasmids expressing either wild-type *RAD53* or the indicated mutations from the native *RAD53* promoter. Assessed after ~100 generations of growth. Only *rad53* mutations exhibiting phenotypes in other assays are shown.

Figure 9 (continued).

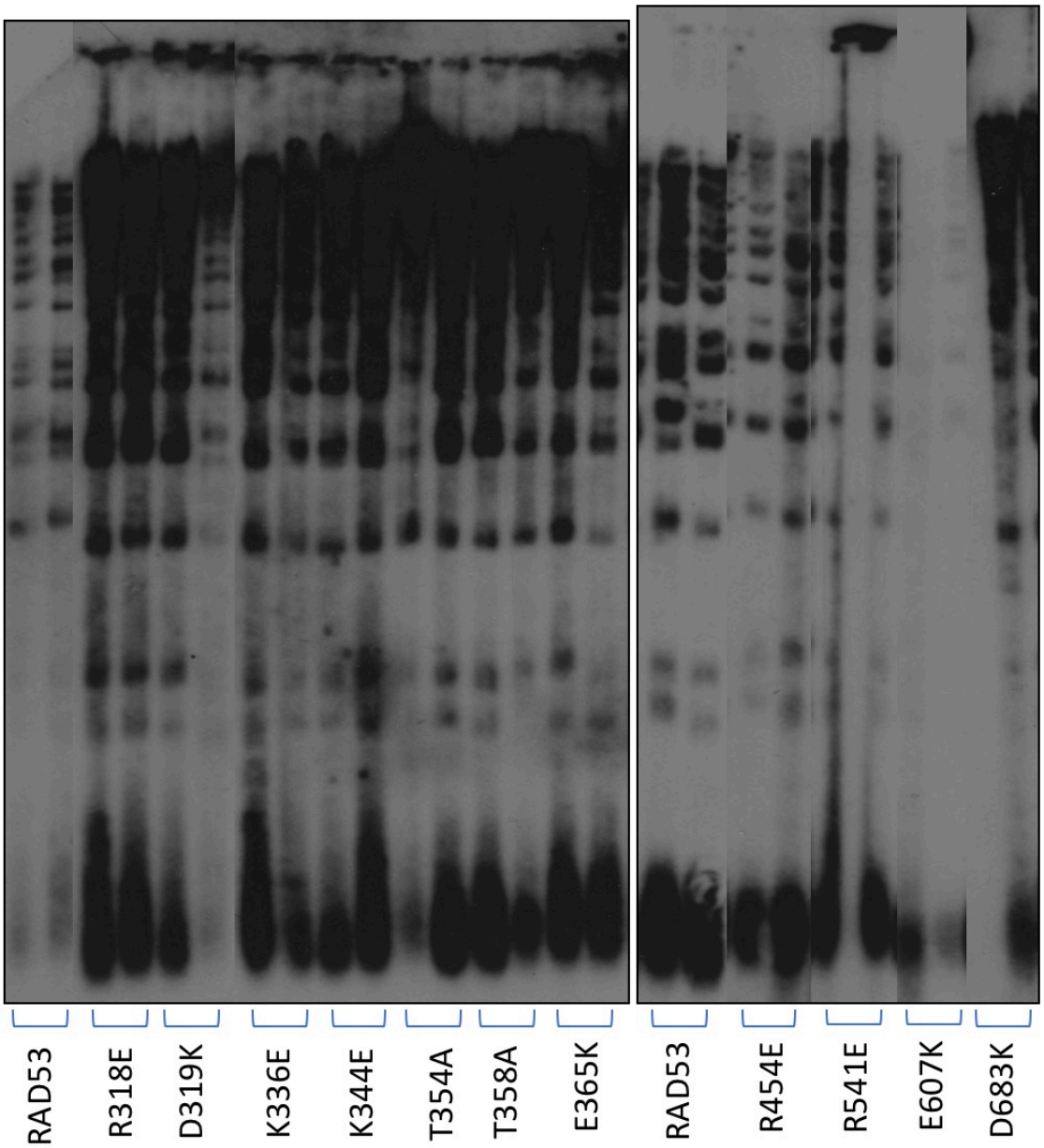

TABLES

Table 1. ODN phenotypes exhibited by *cdc13-ts* yeast strains with *mec1* mutations. Mutations were expressed in high-copy plasmids from an ADH promoter. Yeast strains used were YVL3658 (*cdc13*-S611L) and YVL3660 (*cdc13*-F684S). Strength of the phenotype determined by visual degree of difference in growth compared to the typical growth of most *mec1* mutations. Pictures shown in figure were taken on the third day of growth. Preliminary results.

***mec1* mutation**	**YVL3658 (*cdc13*-S611L)**	**YVL3660 (*cdc13*-F684S)**
E2K	moderately enhanced	moderately enhanced
R217E	slightly enhanced	slightly enhanced
R220E	w.t.	moderately enhanced
C490A	slightly enhanced	moderately enhanced
C493A	slightly enhanced	slightly enhanced
D494K	w.t.	moderately enhanced
R549E	slightly enhanced	moderately enhanced
R582E	w.t.	slightly enhanced
K718E	w.t.	moderately enhanced
K1238E	w.t.	slightly enhanced
K1267E	w.t.	moderately enhanced
K1380E	w.t.	slightly diminished
R1403E	n.t.	moderately enhanced
R1412E	w.t.	moderately enhanced
R1456E	w.t.	slightly enhanced
R1498E	n.t.	slightly diminished
R1652E	w.t.	slightly enhanced
K1671E	w.t.	slightly enhanced
K1839E	w.t.	moderately enhanced
R1845E	slightly enhanced	slightly enhanced
K2063E	w.t.	moderately enhanced
K2080E	w.t.	moderately enhanced
K2081E	w.t.	slightly diminished
R2085E	slightly enhanced	slightly enhanced
R2110E	moderately enhanced	slightly enhanced
R2139E	w.t.	slightly enhanced
K2321E	w.t.	slightly enhanced
K2326E	slightly enhanced	moderately enhanced

Table 2. Phenotypes exhibited by *mec1*-Δ yeast strains with *mec1* mutations resulting from conditions of DNA damage and replication stress from HU, MMS, and 5-FOA. *mec1* mutations were expressed in single-copy plasmids from a native *MEC1* promoter. Strength of the phenotype determined by dosage sensitivity to HU or MMS compared to wild-type sensitivity: "Very strong" if very reduced growth at lower concentrations, "strong" if reduced at lower concentrations, "moderate" if reduced at moderate concentrations, and "slight" if reduced at higher concentrations. Preliminary results.

mec1 mutation	HU phenotype	MMS phenotype	5-FOA phenotype
E158K	strong	strong	close to inviable
W187R	moderate	moderate	w.t.
K678E	w.t.	w.t.	slight
K1259E	w.t.	moderate	w.t.
K1267E	w.t.	w.t.	close to inviable
R1351E	w.t.	moderate	w.t.
R1456E	w.t.	slight	w.t.
R1652E	moderate	strong	w.t.
R1670E	w.t.	w.t.	moderate
R1698E	**very strong**	**very strong**	strong
R1702E	w.t.	moderate	w.t.
K1740E	w.t.	slight	w.t.
K1766E	w.t.	w.t.	slight
R1809E	w.t.	moderate	w.t.
R1845E	strong	moderate	slight
K1850E	**very strong**	**very strong**	slight
R1995E	w.t.	slight	w.t.
K2080E	w.t.	w.t.	moderate
K2081E	w.t.	w.t.	close to inviable
K2109E	n.t.	n.t.	inviable
K2152E	w.t.	w.t.	inviable
R2225E	n.t.	n.t.	inviable

Table 3. Telomere length phenotypes exhibited by *mec1*-Δ yeast strains with *mec1* mutations. *mec1* mutations were expressed in single-copy plasmids from a native *MEC1* promoter.

***mec1* mutation**	**Telomere length phenotype**
R1670E	slightly long
R1702E	slightly short
K2080E	slightly short
K2150E	slightly short

Table 4. ODN phenotypes exhibited by *cdc13-ts* yeast strains with *rad53* mutations. Mutations were expressed in high-copy plasmids from an ADH promoter. Yeast strains used were YVL3658 (*cdc13*-S611L) and YVL3660 (*cdc13*-F684S). Strength of the phenotype determined by visual degree of difference in growth compared to wild-type growth.

*Conflicting results between isolates.

***rad53* mutation**	**YVL3658 (*cdc13*-S611L)**	**YVL3660 (*cdc13*-F684S)**
T5A T8A T12A T15A	w.t.	strongly enhanced
D96K	slightly enhanced	w.t.
D103K	w.t.	slightly enhanced
K115E	slightly diminished	w.t.
D128K	slightly enhanced	slightly enhanced
E129K	moderately enhanced	slightly enhanced
D149K	moderately enhanced	w.t.
K195E	slightly diminished	moderately diminished
K214E	w.t.	strongly enhanced
K227E	moderately enhanced	strongly enhanced
K231E	slightly enhanced	moderately enhanced
E244K	moderately enhanced	moderately enhanced
D280K	moderately enhanced	moderately enhanced
E293K	slightly enhanced	moderately enhanced
D319K	w.t.	moderately enhanced
K321E	w.t.	*slightly enhanced
D323K	w.t.	slightly enhanced
K336E	w.t.	slightly enhanced
D339K	moderately enhanced	moderately enhanced
K344E	w.t.	slightly diminished
T354A	slightly diminished	w.t.
E365K	slightly enhanced	moderately enhanced
D390K	strongly enhanced	strongly enhanced
R454E	w.t.	strongly enhanced
E607K	w.t.	moderately enhanced

Table 5. Phenotypes exhibited by *rad53*-Δ yeast strains with *rad53* mutations resulting from conditions of DNA damage and replication stress from HU, MMS, and 5-FOA. *rad53* mutations were expressed in single-copy plasmids from a native *RAD53* promoter. Strength of the phenotype determined by dosage sensitivity to HU or MMS compared to wild-type sensitivity: "Very strong" if very reduced growth at lower concentrations, "strong" if reduced at lower concentrations, "moderate" if reduced at moderate concentrations, and "slight" if reduced at higher concentrations. Strength of 5-FOA phenotypes determined by visual degree of difference in growth on 5-FOA compared to wild-type growth on 5-FOA. Preliminary results.

*Conflicting results between isolates.

rad53 mutation	HU phenotype	MMS phenotype	5-FOA phenotype
D139K	w.t.	very slight	n.t.
R218E	strong	moderate	w.t.
K227E	w.t.	w.t.	slight
R243E	strong	w.t.	w.t.
E274K	strong	w.t.	w.t.
D280K	strong	w.t.	slight
R318E	**very strong**	w.t.	w.t.
D319K	w.t.	w.t.	*strong
K321E	**very strong**	w.t.	moderate
D323K	w.t.	w.t.	slight
D339K	n.t.	n.t.	***very strong**
K344E	slight	w.t.	w.t.
T354A	moderate	w.t.	w.t.
T358A	moderate	w.t.	w.t.
D390K	n.t.	n.t.	**very strong**
R454E	**very strong**	slight	*strong
R541E	w.t.	slight	w.t.
E607K	w.t.	slight	w.t.
D676K	moderate	very slight	w.t.
D683K	**very strong**	slight	w.t.

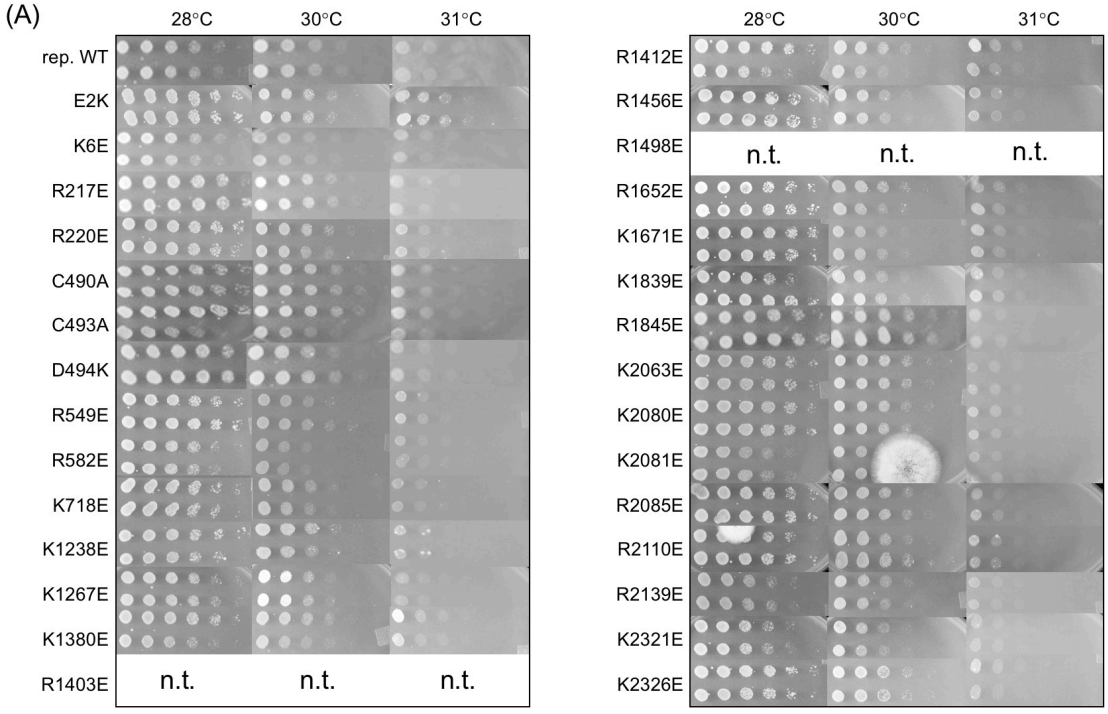

Figure S1. ODN phenotypes exhibited by *cdc13-ts* yeast strains with *mec1* mutations. Growth of *mec1* mutations in yeast strains (A) YVL3658 (*cdc13*-S611L) and (B) YVL3660 (*cdc13*-F684S) at increasingly restrictive temperatures was assessed as described in Figure 4. Pictures shown in figure were taken on the third day of growth. Preliminary results.

Figure S1 (continued).

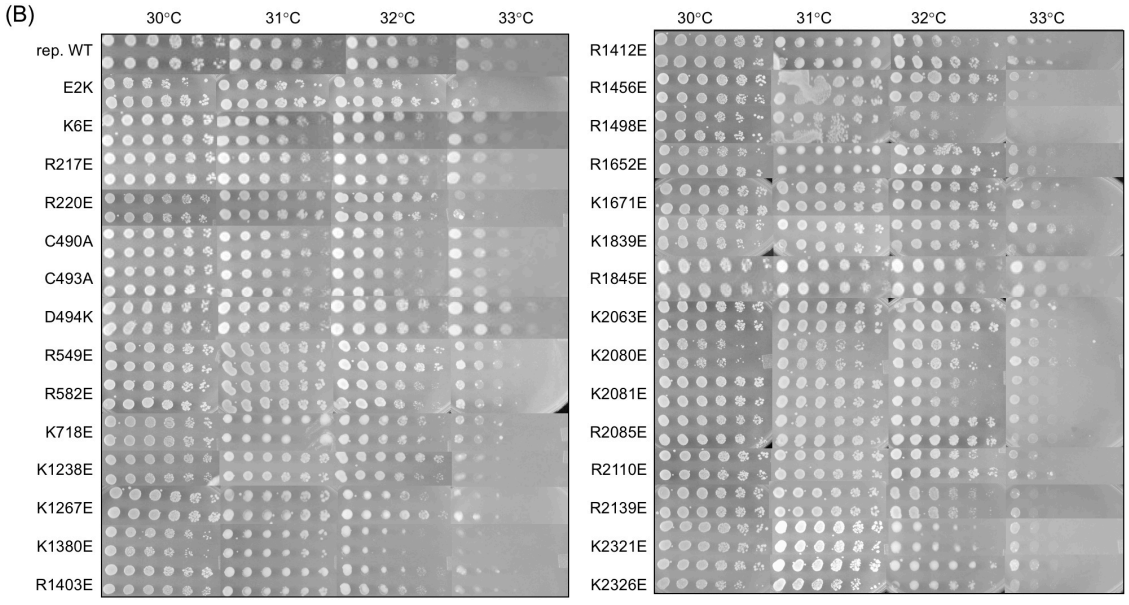

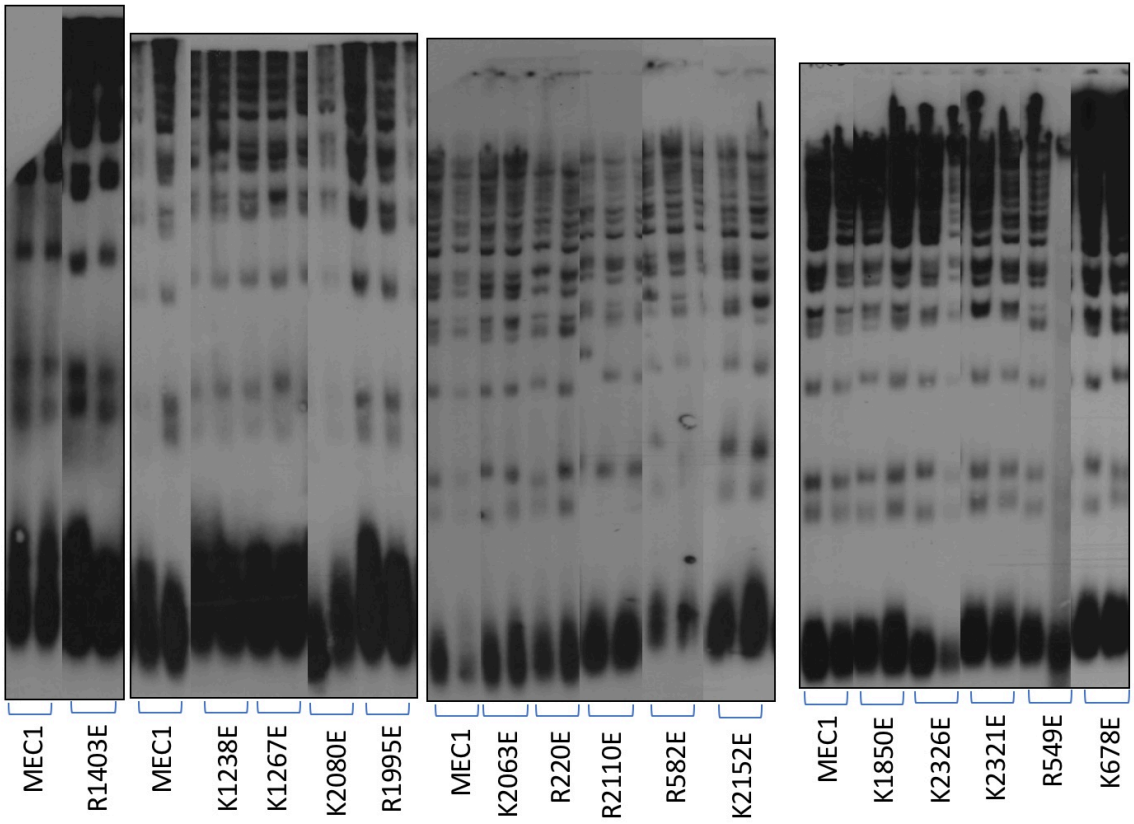

Figure S2. Telomere length analysis of *mec1* mutations. Telomere length of *mec1* mutations in yeast strain YVL5404 (*mec1*-Δ) was assessed as described in Figure 6. Only *mec1* mutations exhibiting phenotypes in other assays are shown.

Figure S2 (continued).

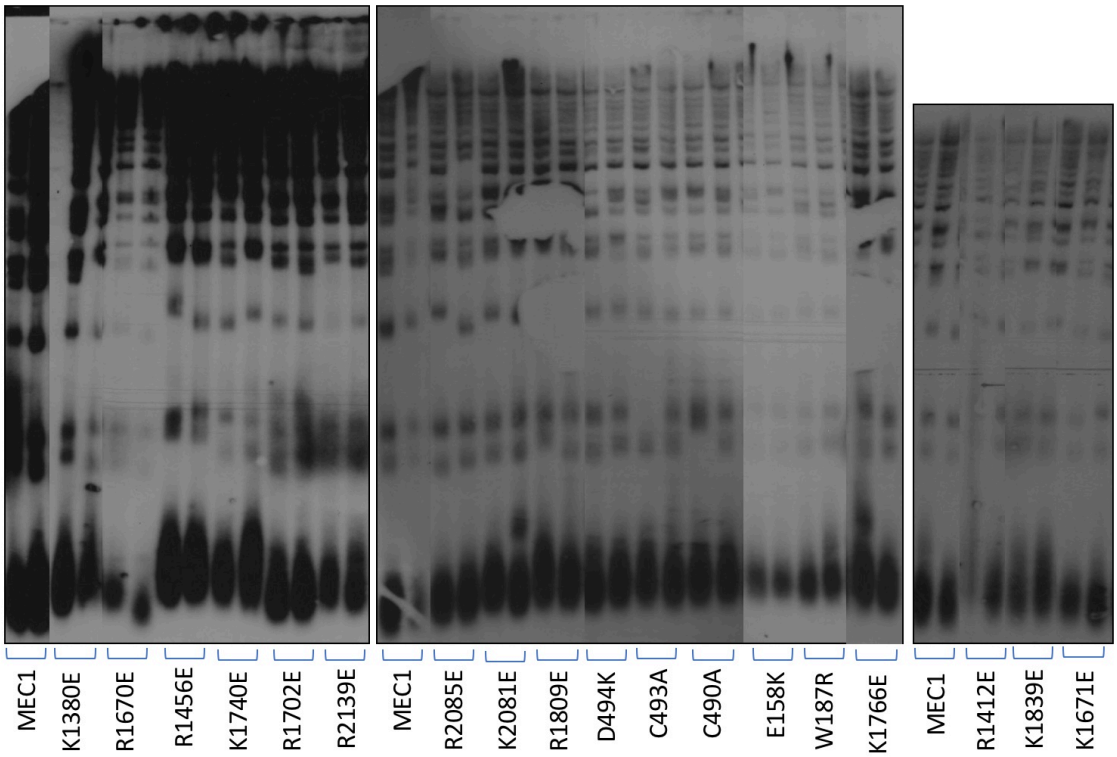

Figure S2 (continued).

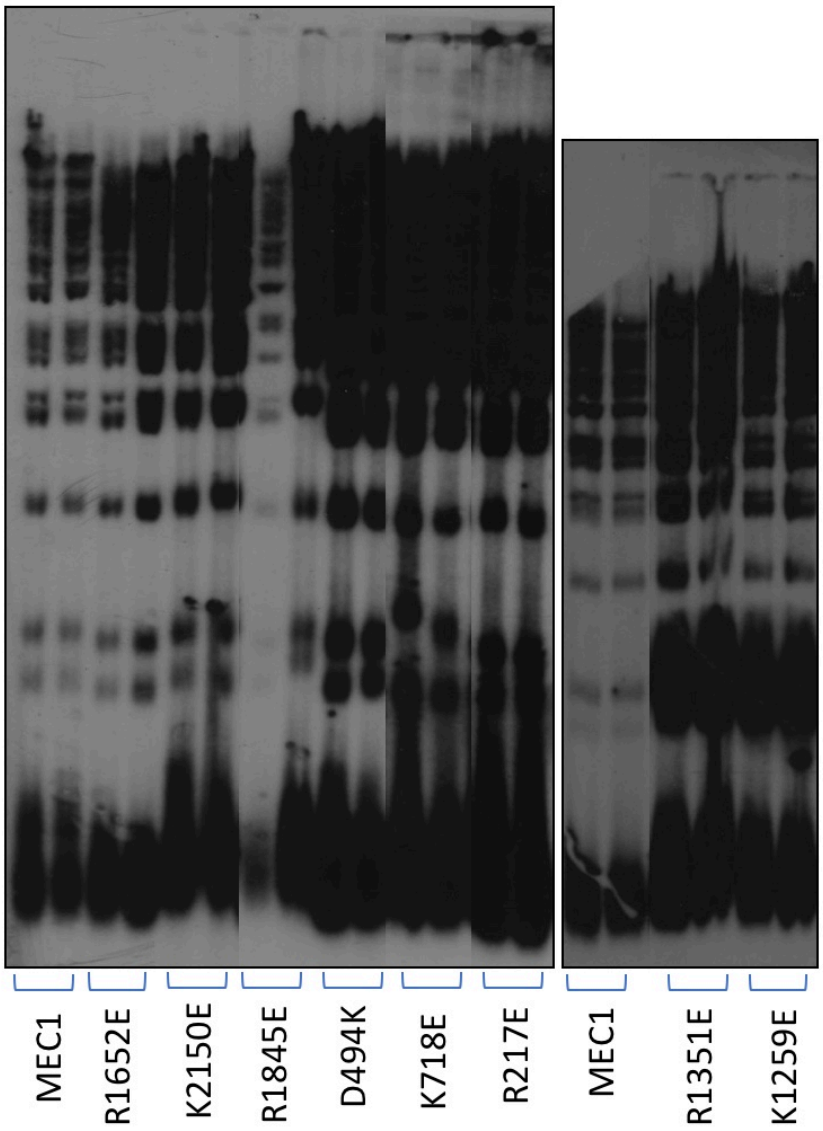

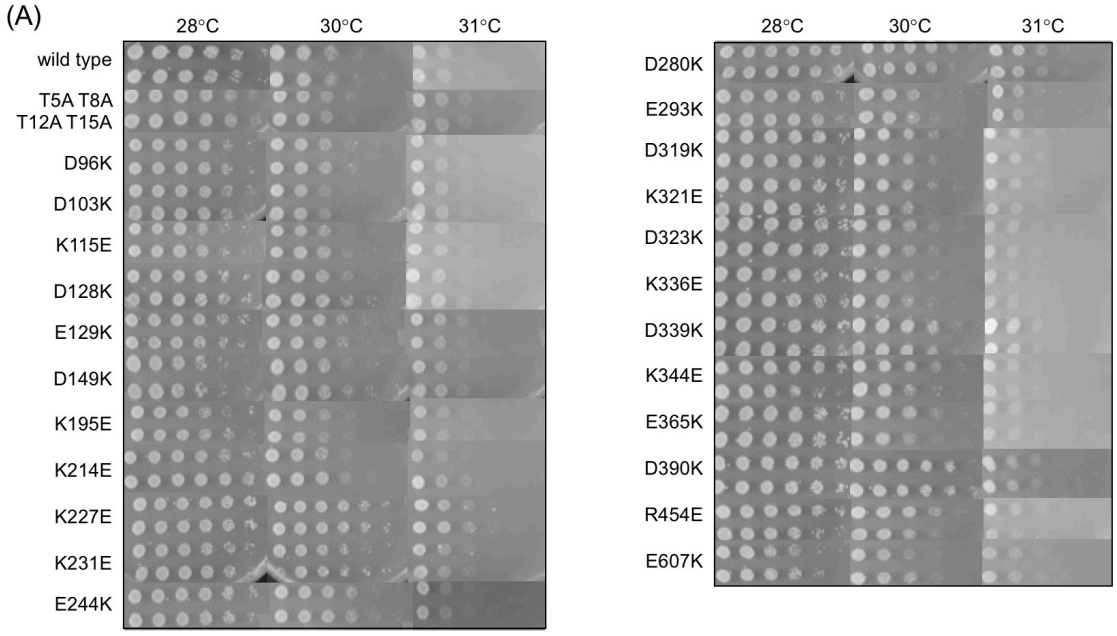

Figure S3. ODN phenotypes exhibited by *cdc13-ts* yeast strains with *rad53* mutations. Growth of *rad53* mutations in yeast strains (A) YVL3658 (*cdc13*-S611L) and (B) YVL3660 (*cdc13*-F684S) at increasingly restrictive temperatures was assessed as described in Figure 7. The Roc- phenotype control used was from a mutation in Rpa1, constructed by Corinne Moeller, a graduate student in the Lundblad lab. Pictures shown in picture were taken on the third day of growth.

Figure S3 (continued).

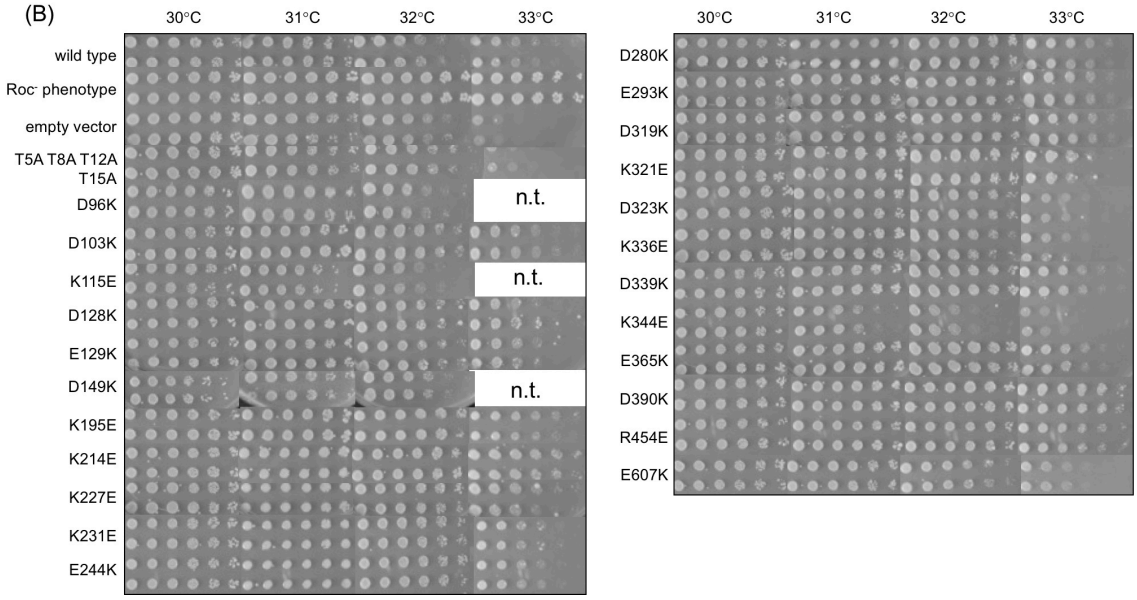

Table S1. Complete list of *mec1* missense mutations.

mec1 mutation	ODN phenotype	HU phenotype	MMS phenotype	5-FOA phenotype	Telomere length phenotype
E2K	moderate	n.t.	n.t.	n.t.	n.t.
K6E	w.t.	w.t.	w.t.	w.t.	w.t.
D9K	w.t.	w.t.	w.t.	w.t.	w.t.
E10K	w.t.	w.t.	w.t.	w.t.	w.t.
K16E	w.t.	w.t.	w.t.	w.t.	w.t.
S37A	w.t.	w.t.	w.t.	w.t.	w.t.
S37D	w.t.	w.t.	w.t.	w.t.	w.t.
S38A	w.t.	w.t.	w.t.	w.t.	w.t.
S38D	w.t.	w.t.	w.t.	w.t.	w.t.
K43E	w.t.	w.t.	w.t.	w.t.	w.t.
K46E	w.t.	w.t.	w.t.	w.t.	w.t.
K72E	w.t.	n.t.	n.t.	n.t.	n.t.
W121R	w.t.	w.t.	w.t.	w.t.	w.t.
W121E	w.t.	w.t.	w.t.	w.t.	w.t.
R124E	w.t.	w.t.	w.t.	w.t.	w.t.
R125E	w.t.	w.t.	w.t.	w.t.	w.t.
K126E	w.t.	w.t.	w.t.	w.t.	w.t.
W130R	w.t.	w.t.	w.t.	w.t.	w.t.
W130E	w.t.	w.t.	w.t.	w.t.	w.t.
K143E	w.t.	w.t.	w.t.	w.t.	w.t.
E158K	w.t.	**strong**	**strong**	close to inviable	w.t.
E170K	w.t.	w.t.	w.t.	w.t.	w.t.
W187R	w.t.	moderate	moderate	w.t.	w.t.
W187E	w.t.	w.t.	w.t.	w.t.	w.t.
D212K	w.t.	w.t.	w.t.	w.t.	w.t.
R217E	moderate	w.t.	w.t.	w.t.	w.t.
R220E	moderate	w.t.	w.t.	w.t.	w.t.
K297E	w.t.	w.t.	w.t.	w.t.	w.t.
R301E	w.t.	n.t.	n.t.	n.t.	n.t.
K341E	w.t.	w.t.	w.t.	w.t.	w.t.
D349K	w.t.	n.t.	n.t.	n.t.	n.t.
K351E	w.t.	w.t.	w.t.	w.t.	w.t.
R352E	w.t.	w.t.	w.t.	w.t.	w.t.
R353E	w.t.	w.t.	w.t.	w.t.	w.t.
E394K	w.t.	w.t.	w.t.	w.t.	w.t.
R397E	w.t.	w.t.	w.t.	w.t.	w.t.

Table S1 (continued).

mec1 mutation	ODN phenotype	HU phenotype	MMS phenotype	5-FOA phenotype	Telomere length phenotype
R427E	w.t.	w.t.	w.t.	w.t.	w.t.
R454E	w.t.	w.t.	w.t.	w.t.	w.t.
C467A	n.t.	w.t.	w.t.	w.t.	n.t.
E469K	w.t.	w.t.	w.t.	w.t.	w.t.
C490A	moderate	w.t.	w.t.	w.t.	w.t.
C493A	moderate	w.t.	w.t.	w.t.	w.t.
D494K	strong	w.t.	w.t.	w.t.	w.t.
R509E	w.t.	w.t.	w.t.	w.t.	w.t.
E537K	w.t.	w.t.	w.t.	w.t.	w.t.
R549E	moderate	w.t.	w.t.	w.t.	w.t.
R582E	slight	w.t.	w.t.	w.t.	w.t.
R585E	w.t.	w.t.	w.t.	w.t.	w.t.
R590E	w.t.	w.t.	w.t.	w.t.	w.t.
K649E	w.t.	w.t.	w.t.	w.t.	w.t.
K678E	w.t.	w.t.	w.t.	slight	w.t.
R693E	w.t.	w.t.	w.t.	w.t.	w.t.
K697E	w.t.	w.t.	w.t.	w.t.	w.t.
K718E	moderate	w.t.	w.t.	w.t.	w.t.
K737E	w.t.	w.t.	w.t.	w.t.	w.t.
K760E	w.t.	w.t.	w.t.	w.t.	w.t.
R769E	w.t.	w.t.	w.t.	w.t.	w.t.
K778E	w.t.	w.t.	w.t.	w.t.	w.t.
K800E	w.t.	w.t.	w.t.	w.t.	w.t.
K811E	w.t.	w.t.	w.t.	w.t.	w.t.
R842E	w.t.	w.t.	w.t.	w.t.	w.t.
K903E	w.t.	w.t.	w.t.	w.t.	w.t.
R905E	w.t.	w.t.	w.t.	w.t.	w.t.
R1031E	w.t.	w.t.	w.t.	w.t.	w.t.
K1104E	w.t.	w.t.	w.t.	w.t.	w.t.
R1106E	w.t.	w.t.	w.t.	w.t.	w.t.
K1130E	w.t.	w.t.	w.t.	w.t.	w.t.
K1176E	w.t.	w.t.	w.t.	w.t.	w.t.
K1189E	w.t.	w.t.	w.t.	w.t.	w.t.
K1215E	w.t.	w.t.	w.t.	w.t.	w.t.
K1221E	w.t.	w.t.	w.t.	w.t.	w.t.
K1238E	slight	w.t.	w.t.	w.t.	w.t.
K1259E	w.t.	w.t.	moderate	w.t.	w.t.

Table S1 (continued).

mec1 mutation	ODN phenotype	HU phenotype	MMS phenotype	5-FOA phenotype	Telomere length phenotype
K1267E	moderate	w.t.	w.t.	close to inviable	w.t.
R1343E	w.t.	w.t.	w.t.	w.t.	w.t.
R1351E	w.t.	w.t.	moderate	w.t.	w.t.
K1357E	w.t.	w.t.	w.t.	w.t.	w.t.
K1358E	w.t.	w.t.	w.t.	w.t.	w.t.
K1380E	slight	w.t.	w.t.	w.t.	w.t.
R1403E	moderate	w.t.	w.t.	w.t.	w.t.
R1412E	moderate	w.t.	w.t.	w.t.	w.t.
R1422E	w.t.	w.t.	w.t.	w.t.	w.t.
R1456E	slight	w.t.	slight	w.t.	w.t.
K1466E	w.t.	w.t.	w.t.	w.t.	w.t.
R1498E	slight	n.t.	n.t.	n.t.	n.t.
K1501E	w.t.	n.t.	n.t.	n.t.	n.t.
K1577E	n.t.	w.t.	w.t.	w.t.	w.t.
K1616E	w.t.	w.t.	w.t.	w.t.	w.t.
R1652E	slight	moderate	strong	w.t.	w.t.
R1670E	w.t.	w.t.	w.t.	moderate	slightly long
K1671E	slight	w.t.	w.t.	w.t.	w.t.
R1698E	w.t.	**very strong**	**very strong**	strong	n.t.
R1702E	w.t.	w.t.	moderate	w.t.	slightly short
K1740E	w.t.	w.t.	slight	w.t.	w.t.
R1760E	w.t.	w.t.	w.t.	w.t.	w.t.
K1766E	w.t.	w.t.	w.t.	slight	w.t.
R1809E	w.t.	w.t.	moderate	w.t.	w.t.
K1839E	moderate	w.t.	w.t.	w.t.	w.t.
R1845E	strong	strong	moderate	slight	w.t.
K1850E	w.t.	**very strong**	**very strong**	slight	w.t.
R1907E	w.t.	w.t.	w.t.	w.t.	w.t.
R1949E	w.t.	w.t.	w.t.	w.t.	w.t.
R1995E	w.t.	w.t.	slight	w.t.	w.t.
K2063E	moderate	w.t.	w.t.	w.t.	w.t.

Table S1 (continued).

mec1 mutation	ODN phenotype	HU phenotype	MMS phenotype	5-FOA phenotype	Telomere length phenotype
K2080E	moderate	w.t.	w.t.	moderate	slightly short
K2081E	slight	w.t.	w.t.	close to inviable	w.t.
R2085E	slight	w.t.	w.t.	w.t.	w.t.
K2103E	w.t.	w.t.	w.t.	w.t.	w.t.
K2109E	w.t.	n.t.	n.t.	inviable	n.t.
R2110E	slight	w.t.	w.t.	w.t.	w.t.
R2123E	w.t.	w.t.	w.t.	w.t.	w.t.
R2139E	slight	w.t.	w.t.	w.t.	w.t.
K2145E	w.t.	w.t.	w.t.	w.t.	w.t.
K2150E	w.t.	w.t.	w.t.	w.t.	slightly short
K2152E	w.t.	w.t.	w.t.	inviable	w.t.
R2203E	w.t.	w.t.	w.t.	w.t.	w.t.
R2208E	w.t.	w.t.	w.t.	w.t.	w.t.
R2225E	w.t.	n.t.	n.t.	inviable	n.t.
K2250E	w.t.	n.t.	n.t.	n.t.	n.t.
R2263E	w.t.	n.t.	n.t.	n.t.	n.t.
K2282E	w.t.	w.t.	w.t.	w.t.	w.t.
R2293E	w.t.	w.t.	w.t.	w.t.	w.t.
K2321E	slight	w.t.	w.t.	w.t.	w.t.
R2324E	w.t.	w.t.	w.t.	w.t.	w.t.
K2326E	moderate	w.t.	w.t.	w.t.	w.t.
R2328E	w.t.	w.t.	w.t.	w.t.	w.t.

Table S2. Complete list of *rad53* missense mutations.

rad53 mutation	ODN phenotype	HU phenotype	MMS phenotype	5-FOA phenotype	Telomere length phenotype
T5A T8A T12A T15A	moderate	n.t.	n.t.	n.t.	n.t.
K63E	w.t.	w.t.	w.t.	w.t.	w.t.
R70E	w.t.	w.t.	w.t.	n.t.	w.t.
R83E	w.t.	w.t.	w.t.	n.t.	w.t.
K87E	w.t.	w.t.	w.t.	n.t.	w.t.
D96K	slight	w.t.	w.t.	n.t.	w.t.
D103K	slight	w.t.	w.t.	w.t.	n.t.
N107E	n.t.	n.t.	n.t.	w.t.	n.t.
N107K	n.t.	n.t.	n.t.	w.t.	n.t.
K115E	slight	w.t.	w.t.	n.t.	w.t.
K118E	w.t.	w.t.	w.t.	n.t.	w.t.
D128K	slight	w.t.	w.t.	n.t.	w.t.
E129K	moderate	w.t.	w.t.	n.t.	w.t.
D139K	w.t.	w.t.	very slight	n.t.	n.t.
D149K	moderate	w.t.	w.t.	n.t.	w.t.
K195E	moderate	w.t.	w.t.	n.t.	w.t.
D196K	w.t.	w.t.	w.t.	n.t.	w.t.
E202K	w.t.	w.t.	w.t.	n.t.	w.t.
K213E	w.t.	w.t.	w.t.	n.t.	w.t.
K214E	strong	w.t.	w.t.	n.t.	w.t.
E217K	w.t.	w.t.	w.t.	n.t.	w.t.
R218E	w.t.	strong	moderate	w.t.	w.t.
K227E	strong	w.t.	w.t.	slight	w.t.
K231E	moderate	w.t.	w.t.	n.t.	w.t.
R232E	w.t.	w.t.	w.t.	n.t.	w.t.
K233E	w.t.	w.t.	w.t.	n.t.	w.t.
R243E	w.t.	strong	w.t.	w.t.	w.t.
E244K	moderate	w.t.	w.t.	n.t.	w.t.
N252E	n.t.	n.t.	n.t.	w.t.	n.t.
N252K	n.t.	n.t.	n.t.	w.t.	n.t.
K260E	w.t.	n.t.	n.t.	w.t.	n.t.
E264K	w.t.	w.t.	w.t.	n.t.	w.t.
D265K	w.t.	w.t.	w.t.	n.t.	w.t.
E274K	w.t.	strong	w.t.	w.t.	w.t.
D280K	moderate	strong	w.t.	slight	w.t.
E293K	moderate	w.t.	w.t.	n.t.	w.t.

Table S2 (continued).

rad53 mutation	ODN phenotype	HU phenotype	MMS phenotype	5-FOA phenotype	Telomere length phenotype
D294K	w.t.	w.t.	w.t.	n.t.	w.t.
R318E	w.t.	**very strong**	w.t.	w.t.	w.t.
D319K	moderate	w.t.	w.t.	strong	w.t.
K321E	slight	**very strong**	w.t.	moderate	n.t.
D323K	slight	w.t.	w.t.	slight	n.t.
K336E	slight	w.t.	w.t.	n.t.	w.t.
D339K	moderate	n.t.	n.t.	**very strong**	n.t.
K344E	slight	slight	w.t.	w.t.	w.t.
T354A	w.t.	moderate	w.t.	w.t.	w.t.
T358A	w.t.	moderate	w.t.	w.t.	w.t.
E365K	moderate	w.t.	w.t.	w.t.	w.t.
Y385E	w.t.	w.t.	w.t.	n.t.	w.t.
Y385K	w.t.	w.t.	w.t.	n.t.	w.t.
D390K	**very strong**	n.t.	n.t.	**very strong**	n.t.
H405E	w.t.	w.t.	w.t.	n.t.	w.t.
H405K	w.t.	w.t.	w.t.	n.t.	w.t.
R422E	w.t.	w.t.	w.t.	n.t.	w.t.
Y425E	w.t.	w.t.	w.t.	n.t.	w.t.
Y425K	w.t.	w.t.	w.t.	n.t.	w.t.
E427K	w.t.	w.t.	w.t.	n.t.	w.t.
E437K	w.t.	w.t.	w.t.	n.t.	n.t.
E438K	w.t.	w.t.	w.t.	w.t.	w.t.
D441K	w.t.	w.t.	w.t.	n.t.	w.t.
D450K	w.t.	w.t.	w.t.	n.t.	w.t.
R454E	strong	**very strong**	slight	strong	w.t.
K459E	w.t.	w.t.	w.t.	n.t.	w.t.
S480A S485A S489A	w.t.	n.t.	n.t.	n.t.	n.t.
R541E	w.t.	w.t.	slight	w.t.	w.t.
R605E	w.t.	w.t.	w.t.	n.t.	w.t.
E607K	slight	w.t.	slight	w.t.	w.t.

Table S2 (continued).

rad53 mutation	ODN phenotype	HU phenotype	MMS phenotype	5-FOA phenotype	Telomere length phenotype
D615K	w.t.	w.t.	w.t.	n.t.	w.t.
R617E	w.t.	w.t.	w.t.	n.t.	w.t.
R620E	w.t.	n.t.	n.t.	w.t.	n.t.
K627E	w.t.	w.t.	w.t.	n.t.	w.t.
E638K	n.t.	w.t.	w.t.	n.t.	w.t.
D645K	w.t.	w.t.	w.t.	n.t.	w.t.
D646K	w.t.	w.t.	w.t.	w.t.	n.t.
D676K	w.t.	moderate	very slight	w.t.	n.t.
D683K	w.t.	**very strong**	slight	w.t.	w.t.
D698K	n.t.	w.t.	w.t.	n.t.	w.t.
R714E	w.t.	w.t.	w.t.	n.t.	w.t.
E722K	n.t.	w.t.	w.t.	n.t.	w.t.
E723K	w.t.	w.t.	w.t.	n.t.	w.t.
K785E	w.t.	w.t.	w.t.	n.t.	w.t.
R786E	w.t.	w.t.	w.t.	n.t.	w.t.
K801E	w.t.	w.t.	w.t.	n.t.	w.t.
K802E	w.t.	w.t.	w.t.	n.t.	w.t.
K804E	w.t.	w.t.	w.t.	n.t.	w.t.
R805E	w.t.	w.t.	w.t.	n.t.	w.t.

DISCUSSION

The results of my genetic screens of Mec1 and Rad53 have revealed a number of highly conserved, hydrophobic amino acids on the surfaces of each protein that may be important in DNA damage pathways of the S-phase checkpoint. My use of the overexpression dominant-negative (ODN) mutagenesis assay to facilitate generation of a functional surface map of Mec1 and Rad53 was especially effective when used in conjunction with variations of traditional loss-of-function (LOF) mutagenesis assays; testing the effects of each mutation on the cell's ability to respond to different types of DNA damage and replication stress will help further our understanding of these DNA damage pathways. From my mutagenesis, I have identified a number of mutations conferring strong ODN phenotypes, some of which are present in clusters of other residues conferring ODN phenotypes. I have also identified a number of mutations showing heightened sensitivity to DNA damaging agents such as hydroxyurea (HU), methyl methanesulfonate (MMS), and 5-fluoro-orotic acid (5-FOA), indicating potential sites of interaction between Mec1 or Rad53 and other proteins involved in the S-phase checkpoint.

My genetic screens of Mec1 and Rad53 have thus laid a foundation for furthering our understanding of the S-phase checkpoint. Use of the ODN mutagenesis assay has allowed me to identify potential functionally important surface residues, the study of which can reveal details about the mechanisms by which Mec1 and Rad53 operate in DNA damage response pathways. Following

integration of the 28 *mec1* mutations and the 25 *rad53* mutations into the *S. cerevisiae* genome, I can determine whether these mutations truly confer an ODN or Roc$^-$ phenotype and proceed with finding surface residues on other proteins involved in the pathways that, when mutated alongside the *mec1* or *rad53* mutation, show a significantly enhanced effect on biochemical activity. Other members in the Lundblad lab have also conducted ODN mutagenesis screens in other proteins in the S-phase checkpoint; the addition of my findings to the functional surface maps generated for each protein will help further our understanding of the DNA damage response pathways.

Additionally, use of LOF mutagenesis assays testing the effects of *mec1* or *rad53* mutations on cell viability in conditions of DNA damage and replication stress has allowed for the identification of mutations that potentially disrupt essential biochemical activity of Mec1 or Rad53, respectively. Certain mutations put through the synthetic lethality assays show enhanced sensitivity to HU, MMS, or 5-FOA. The surface residues affected could, like in the ODN mutagenesis screens, be potential sites of interaction between proteins essential in the overall response to DNA damage or replication stress. Because of technical issues in the HU and MMS assays as well as incomplete 5-FOA data, the first steps in investigating the affected surface residues is to re-test the *mec1* and *rad53* mutations in the synthetic lethality assays and to integrate these mutations into the genome. After determining whether these mutations truly affect cell viability in

unfavorable conditions, I can begin investigating the significance of these residues to the roles of Mec1 and Rad53 in the S-phase checkpoint.

My telomere length analysis of Mec1 and Rad53 revealed a few *mec1* mutations with only very slight effects on telomere length compared to that of the wild type. However, other studies into the roles of Mec1 and have shown that they are important in various areas of telomere regulation; while both proteins are critical to inhibiting ssDNA production at telomeres in cells with defects in telomere maintenance (46), Mec1 is particularly important to maintaining wild-type telomere length (47). As a result, conducting a second telomere length assay of mutations in Mec1 and Rad53 could lead to identification of missed sites of interaction between proteins involved in telomere length regulation.

As discussed earlier, both DNA damage response pathways in the S-phase checkpoint rely on Mec1 and Rad53 but work through separate mediator proteins. The DNA damage checkpoint (DDC) pathway works through mediator protein Rad9, while the DNA response checkpoint (DRC) pathways works through mediator protein Mrc1 (11). In comparison to the DDC, details about how the DRC operates mechanistically remain poorly understood; however, Rad53 is known to promote the stabilization of DNA replication forks (11). As a result, activation of Rad53 and its associated kinases are critical to activation of the DRC pathway. Additionally, Mec1 and Mrc1 are present at stalled replication forks during Rad53 recruitment (27). Studies have shown that Mrc1 facilitates the accumulation of Mec1 at stalled forks as well as the recruitment and subsequent phosphorylation

of Rad53 (48). Rad53 activation is also much more efficient when both Mec1 and Mrc1 are present as opposed to when Mec1 acts alone; when Rad53 is limited in concentration, Mec1 and Mrc1 are equally important upstream factors in activating Rad53 (27). These findings suggest that in the DRC, Mec1 and Mrc1 are critical to the kinase cascade that leads to activation of Rad53; however, the mechanistic details of the DRC and the specific role of Mrc1 in the DRC remain poorly understood (27). By employing the same assays used in testing *mec1* and *rad53* mutations to test mutations in Mrc1, I can generate a functional surface map that can help further our understanding of how Mrc1 operates in the DRC and S-phase checkpoint. Through such an investigation of Mrc1, the differences between the DDC and DRC that determine which pathway to use in conditions of DNA damage and replication stress can be elucidated. Understanding why one pathway activates over another in these conditions could greatly facilitate the development of future treatments of cancer and other genetic diseases.

REFERENCES

(1). Lengauer C, Kinzler KW, Vogelstein B. (1998). Genetic instabilities in human cancers. *Nature*. 396:643-9.

(2). Hartwell, L. (1992). Defects in a cell cycle checkpoint may be responsible for the genomic instability of cancer cells. *Cell*. 71:543-46.

(3). Nowell, PC. (1976). The clonal evolution of tumor cell populations. *Science*. 194:23-8.

(4). Pikor L, Thu K, Vucic E, Lam W. (2013). *Cancer Metastasis Rev.* 32:341-52.

(5). Friedberg, EC. (2008). A brief history of the DNA repair field. *Cell Res.* 18:3-7.

(6). Kim N, Jinks-Robertson S. (2012). Transcription as a source of genome instability. *Nat Rev Genet.* 13:204-14.

(7). Haber, JE. (2015). Deciphering the DNA damage response. *Cell*. 162:1183-5.

(8). Técher H, Koundrioukoff S, Nicolas A, Debatisse M. (2017). The impact of replication stress on replication dynamics and DNA damage in vertebrate cells. *Nat Rev Genet.* 18:535-50.

(9). Friedel AM, Pike BL, Gasser SM. (2009). ATR/Mec1: coordinating fork stability and repair. *Curr Opin Cell Biol*. 21:237-244.

(10). Paulovich AG, Hartwell LH (1995). A checkpoint regulates the rate of progression through S phase in *S. cerevisiae* in response to DNA damage. *Cell*. 82:841-7.

(11). Pardo B, Crabbé L, Pasero P. (2017). Signaling pathways of replication stress in yeast. *FEMS Yeast Res*. 17. fow101.

(12). Segurado M, Tercero JA. (2009). The S-phase checkpoint: targeting the replication fork. *Biol Cell*. 101:617-27.

(13). Duina AA, Miller ME, Keeney JB. (2014). Budding yeast for budding geneticists: a primer on the *Saccharomyces cerevisiae* model system. *Genetics*. 197:33-48.

(14). Johnston M. (1996). Genome sequencing: The complete code for a eukaryotic cell. *Curr Biol*. 6:500-3.

(15). Botstein D, Chervitz SA, Cherry JM. (1997). Yeast as a model organism. *Science*. 277:1259-60.

(16). Kanaar R, Troelstra C, Swagemakers SMA, Essers J, Smit B, Franssen J-H, Pastink A, Bezzubova OY, Buerstedde J-M, Clever B, Heyer W-D, Hoeijmakers JHJ. (1996). Human and mouse homologs of the *Saccharomyces cerevisiae RAD54* DNA repair gene: evidence for functional conservation. *Curr Biol.* 6:828-38.

(17). Jiang JC, Kirchman PA, Zagulski M, Hunt J, Jazwinski SM. (1998). Homologs of the yeast longevity gene *LAG1* in *Caenorhabditis elegans* and human. *Genome Res.* 8:1259-72.

(18). Strand M, Prolla TA, Liskay RM, Petes TD. (1993). Destabilization of tracts of simple repetitive DNA in yeast by mutations affecting DNA mismatch repair. *Nature*. 365:274-6.

(19). Segurado M, Diffley JFX. (2008). Separate roles for the DNA damage checkpoint protein kinases in stabilizing DNA replication forks. *Genes Dev*. 22:1816-27.

(20). Osborn AJ, Elledge SJ. (2003). Mrc1 is a replication fork component whose phosphorylation in response to DNA replication stress activates Rad53. *Genes Dev*. 17:1755-67.

(21). Branzei D, Foiani M. (2006). The Rad53 signal transduction pathway: Replication fork stabilization, DNA repair, and adaptation. *Exp Cell Res*. 312:2654-59.

(22). Puddu F, Piergiovanni G, Plevani P, Muzi-Falconi M. (2011). Sensing of replication stress and Mec1 activation act through two independent pathways involving the 9-1-1 complex and DNA polymerase ε. *PLoS Genet*. 7. e1002022.

(23). Ciccia A, Elledge SJ. (2010). The DNA damage response: making it safe to play with knives. *Mol Cell*. 40:179-204.

(24). Sweeney FD, Yang F, Chi A, Shabanowitz J, Hunt DF, Durocher D. (2005). *Saccharomyces cerevisiae* Rad9 acts as a Mec1 adaptor to allow Rad53 activation. *Curr Biol.* 15:1364-75.

(25). Alcasabas AA, Osborn AJ, Bachant J, Hu F, Werler PJH, Bousset K, Furuya K, Diffley JFX, Carr AM, Elledge SJ. (2001). Mrc1 transduces signals of DNA replication stress to activate Rad53. *Nat Cell Biol.* 3:958-65.

(26). Shimada K, Pasero P, Gasser SM. (2002). ORC and the intra-S-phase checkpoint: athreshold regulates Rad53p activation in S phase. *Genes Dev.* 16:3236-52.

(27). Chen SH, Zhou H. (2009). Reconstitution of Rad53 activation by Mec1 through adaptor protein Mrc1. *J Biol Chem*. 284:18593-603.

(28). Zhao X, Muller EGD, Rothstein R. (1998). A suppressor of two essential checkpoint genes identifies a novel protein that negatively affects dNTP pools. *Mol Cell*. 2:329-40.

(29). Mushegian AR, Koonin EV. (1996). A minimal gene set for cellular life derived by comparison of complete bacterial genomes. *Proc Natl Acad Sci USA*. 93:10268-73.

(30). Lubin JW, Rao T, Mandell EK, Wuttke DS, Lundblad V. (2013). Dissecting protein function: an efficient protocol for identifying separation-of-function mutations that encode structurally stable proteins. *Genetics*. 193:715-25.

(31). Schiestl RH, Roberts JD, Zakour RA. (1989). High efficiency transformation of intact yeast cells using single stranded nucleic acids as a carrier. *Curr Genet*. 16:339-346.

(32). Guthrie C, Fink GR. *Guide to Yeast Genetics and Molecular Biology*. San Diego, Academic Press. 1991.

(33). Petermann E, Orta ML, Issaeva N, Schultz N, Helleday T. (2010). Hydroxyurea-stalled replication forks become progressively inactivated and require two different RAD51-mediated pathways for restart and repair. *Mol Cell*. 37:492-502.

(34). Lundin C, North M, Erixon K, Walters K, Jenssen D, Goldman ASH, Helleday T. (2005). Methyl methanesulfonate (MMS) produces heat-labile DNA damage but no detectable *in vivo* DNA double-strand breaks. *Nucleic Acids Res*. 33:3799-811.

(35). Boeke JD, Trueheart J, Natsoulis G, Fink GR. (1987). 5-Fluoroorotic acid as a selective agent in yeast molecular genetics. *Methods Enzymol.* 154:164 75.

(36). Ben-Aroya S, Coombes C, Kwok T, O'Donnell KA, Boeke JD, Hieter P. (2008). Toward a comprehensive temperature-sensitive mutant repository of the essential genes of *Saccharomyces cerevisiae*. *Mol Cell*. 30:248-258.

(37). Venkatesen K, Rual JF, Vazquez A, Stelzl U, Lemmens I, Hirozane Kishikawa T, Hao T, Zenkner M, Xin X, Goh KI, Yildirim MA, Simonis N, Heinzmann K, Gebreab F, Sahalie JM, Cevik S, Simon C, de Smet AS, Dann E, Smolyar A, Vinayagam A, Yu H, Szeto D, Borick H, Dricot A, Klitgord N, Murray RR, Lin C, Lalowski M, Timm J, Rau K, Boone C, Braun P, Cusick ME, Roth FP, Hill DE, Tavernier J, Wanker EE, Barabasi AL, Vidal M. (2009). An empirical framework for binary interactome mapping. *Nat Methods*. 6:83-90.

(38). Constanzo M, Baryshnikova A, Bellay J, Kim Y, Spear ED, Sevier CS, Ding H, Koh JL, Toufighi K, Mostafavi S, Prinz J, St. Onge RP, VanderSluis B, Makhnevych T, Vizeacoumar FJ, Alizadeh S, Bahr S, Brost RL, Chen Y, Cokol M Deshpande R, Li Z, Lin ZY, Liang W, Marback M, Paw J, San Luis BJ, Shuteriqi E, Tong AH, van Dyk N, Wallace IM, Whitney JA, Weirauch MT, Zhong G, Zhu H, Houry WA, Brudno M, Ragibizadeh S, Papp B, Pal C, Roth FP, Giaever G, Nislow C, Troyanskaya OG, Bussey H, Bader GD, Gingras AC, Morris QD, Kim PM, Kaiser CA, Myers CL, Andrews BJ, Boone C. (2010). The genetic landscape of a cell. *Science*. 327:425-31.

(39). Lim WA, Farruggio DC, Sauer RT. (1992). Structural and energetic consequences of disruptive mutations in a protein core. *Biochemistry*. 31:4324-4333.

(40). Wells JA. (1991). Systematic mutational analyses of protein-protein interfaces. *Methods Enzymol*. 202:390-411.

(41). Hardy S, Legagneux V, Audic Y, Paillard L. (2010). Reverse genetics in eukaryotes. *Biol Cell*. 102:561-80.

(42). Lubin JW, Tucey TM, Lundblad V. (2018). Using separation-of-function mutagenesis to define the full spectrum of activities performed by the Est1 telomerase subunit *in vivo*. *Genetics*. 208:97-110.

(43). Collins SR, Miller KM, Maas NL, Roguev A, Fillingham J, Chu CS, Schuldiner M, Gebbia M, Recht J, Shales M, Ding H, Xu H, Han J, Ingvarsdottir K, Cheng B, Andrews B, Boone C, Berger SL, Hieter P, Zhang Z, Brown GW, Ingles CJ, Emili A, Allis CD, Toczyski DP, Weissman JS, Greenblatt JF, Krogan NJ. (2007). Functional dissection of protein complexes involved in yeast chromosome biology using a genetic interaction map. *Nature*. 446:806-10.

(44). Breslow DK, Cameron DM, Collins SR, Schuldiner M, Stewart-Ornstein J, Newman HW, Braun S, Madhani HD, Krogan NJ, Weissman JS. (2008). A comprehensive strategy enabling high resolution functional analysis of the yeast genome. *Nat Methods*. 5:711-18.

(45). Paschini M, Toro TB, Lubin JW, Braunstein-Ballew B, Morris DK, Lundblad V. (2012). A naturally thermolabile activity compromises genetic analysis of telomere function in *Saccharomyces cerevisiae*. *Genetics*. 191:79-93.

(46). Jia X, Weinert T, Lydall D. (2003). Mec1 and Rad53 inhibit formation of single stranded DNA at telomeres of *Saccharomyces cerevisiae cdc13-1* mutants. *Genetics*. 166:753-64.

(47). Ritchie KB, Mallory JC, Petes TD. (1999). Interactions of *TLC1* (which encodes the RNA subunit of telomerase), *TEL1*, and *MEC1* in regulating telomere length in the yeast *Saccharomyces cerevisiae*. *Mol Cell*. 19:6065 75.

(48). Naylor ML, Li J, Osborn AJ, Elledge SJ. (2009). Mrc1 phosphorylation in response to DNA replication stress is required for Mec1 accumulation at the stalled fork. *Proc Natl Acad Sci U S A*. 106:12765-70.